Diploma Thesis

Optimising Large-Scale PEM Electrolysis for Green Hydrogen Production: A Comprehensive Techno-Economic Case Study

within the study programme

Physikalische Energie- und Messtechnik
(Physical Energy and Measurement Engineering)

by

Natalie Frassl
11902096

Supervision
Univ.Prof. Dipl.-Ing. Dr.techn. Markus Valtiner (TU Wien / Institut für Angewandte Physik)
Dr. Yannick Wimmer (AIT Austrian Institute of Technology GmbH / Power and Renewable Gas Systems)

Vienna, December 10, 2024

(Signature Author) (Signature Supervisor)

Abstract

Green hydrogen is emerging as a crucial energy carrier in clean energy systems, vital for mitigating the volatility of renewable sources. Proton Exchange Membrane (PEM) electrolysis, providing a fast dynamic response, is well-suited for hydrogen production, though it generates substantial waste heat.

This study investigates the techno-economic potential of a large-scale PEM electrolyser powered by renewable energy, focusing on green hydrogen production. System configurations are varied, including adjustments to electrolyser, wind, and photovoltaic capacities, and operational strategies. Additionally, the feasibility of waste heat utilisation for a local district heating network is explored for possible efficiency gain. A verified PEM model is implemented into a renewable energy simulation framework to evaluate key metrics, both technical and economic.

Results indicate that optimal system configurations involve a high share of installed renewable energy generation relative to electrolyser capacity. Furthermore, waste heat recovery has the potential to enhance stack efficiency by nearly 20 % points. The estimated Levelised Cost of Hydrogen ranges from 4.2-4.8 €/kg under ideal scenarios, with the more cost-effective strategy considering fluctuating electricity purchases from the grid. These findings highlight that green hydrogen faces challenges in competing with fossil-based hydrogen on a global scale, even under optimistic capital cost assumptions. In this study, utilising waste heat for district heating results in only minor reductions of hydrogen production costs, whereas full reuse of the useable excess heat could offer more substantial savings. Moreover, the viability of waste heat supply is contingent on the required temperature level, with heat pumps playing a crucial role.

In conclusion, while PEM electrolysis demonstrates considerable potential for green hydrogen production, further cost reductions are essential if it is to compete globally with grey hydrogen. Achieving competitiveness will rely on advancements in PEM technology and reductions in capital expenditures. Research into waste heat recovery and optimising electricity procurement could further help to reduce production costs and create a viable, sustainable alternative to fossil fuel-derived hydrogen.

Keywords: Proton Exchange Membrane Electrolysis; Techno-Economic Analysis; Green Hydrogen; Waste Heat Recovery; Renewable Energy System; Modelling

Kurzfassung

Grüner Wasserstoff entwickelt sich zu einem wichtigen Energieträger in nachhaltigen Energiesystemen und spielt eine entscheidende Rolle bei der Ausbalancierung von erneuerbaren Energiequellen. Die Protonen-Austausch-Membran-Elektrolyse (PEM), welche eine schnelle dynamische Reaktion ermöglicht, eignet sich besonders gut für Wasserstoffproduktion, obwohl sie erhebliche Abwärme erzeugt.
Diese Studie untersucht das techno-ökonomische Potenzial eines großen PEM-Elektrolyseurs, der mit erneuerbarer Energie betrieben wird, der Fokus wird hierbei auf die Produktion von grünem Wasserstoff gelegt. Es werden verschiedene Systemkonfigurationen analysiert, einschließlich Anpassungen der Kapazitäten für Elektrolyseur, Wind- und Photovoltaikanlagen sowie Betriebsstrategien. Zusätzlich wird die Machbarkeit der Abwärmenutzung für ein lokales Wärmenetz zur Effizienzsteigerung untersucht. Ein verifiziertes PEM-Modell wird in eine Simulationssoftware für erneuerbare Energien integriert, um wichtige technische und ökonomische Kennzahlen zu bewerten.
Die Ergebnisse zeigen, dass die optimalen Systemkonfigurationen hohe Anteile an installierter erneuerbarer Energie im Vergleich zur Elektrolyseurkapazität aufweisen. Darüber hinaus hat Abwärmerückgewinnung das Potenzial, die Effizienz des Elektrolyseurs um fast 20 % Punkte zu steigern. Die berechneten Kosten für die Wasserstoffproduktion liegen unter idealen Bedingungen bei 4.2-4.8 €/kg, wobei die kostengünstigste Variante fluktuierende Stromkäufe aus dem Netz berücksichtigt. Diese Ergebnisse verdeutlichen, dass grüner Wasserstoff auf globaler Ebene noch Schwierigkeiten hat, mit fossilem Wasserstoff zu konkurrieren, selbst unter optimistischen Annahmen zu den Investitionskosten. In dieser Studie führt die Nutzung von Abwärme für Fernwärme nur zu geringen Reduzierungen der Wasserstoffproduktionskosten, während die vollständige Nutzung der überschüssigen Abwärme größere Einsparungen ermöglichen könnte. Darüber hinaus ist die Rentabilität der Abwärmenutzung von der erforderlichen Temperatur abhängig, wobei Wärmepumpen eine entscheidende Rolle spielen.
Abschließend zeigt die Studie, dass PEM-Elektrolyse ein erhebliches Potenzial für die Produktion von grünem Wasserstoff aufweist, jedoch weitere Kostenreduktionen erforderlich sind, um auf globaler Ebene mit grauem Wasserstoff konkurrenzfähig werden zu können. Die Erreichung der Wettbewerbsfähigkeit hängt von Fortschrit-

ten in der PEM-Technologie und der Senkung der Investitionskosten ab. Forschungen zur Abwärmenutzung und zur Optimierung des Strombezugs könnten ebenfalls dazu beitragen, die Produktionskosten weiter zu verringern und grünen Wasserstoff zu einer nachhaltigen Alternative zu fossilem Wasserstoff zu machen.

Schlüsselwörter: PEM-Elektrolyse; Techno-ökonomische Analyse; grüner Wasserstoff; Abwärmenutzung; Erneuerbares Energiesystem; Modellierung

Acknowledgements

This thesis was financially supported by the project *H2REAL* (FO999894621), funded by the Climate and Energy Fund, during my time at the Austrian Institute of Technology GmbH (AIT).

I am deeply grateful to my supervisor, Yannick, for his unwavering support and guidance throughout this work. He was always approachable when I needed help, provided thoughtful advice, and created a positive, joyful and productive working environment. His openness to my ideas, even when they did not align with his initial views, was especially encouraging.
My sincere thanks also go to my colleagues at AIT, whose support, advice, and camaraderie made my time there both enriching and enjoyable. Some elements of my thesis were made possible thanks to their earlier work and their presence turned the office into a place I genuinely looked forward going to.
I would like to express my appreciation to Prof. Valtiner from TU Wien for his expert guidance. His insights and support were invaluable during my thesis journey.

Lastly, a heartfelt thank you to my family and friends for their continued support throughout my studies, always providing a listening ear and uplifting words. I am particularly grateful to my parents for their financial aid, which enabled me to focus on my academic pursuits. They continually encouraged me to pursue my passion for science, with my dad's influence being especially pivotal.

Nomenclature

Abbreviations

AEL	Alkaline Electrolyser
BoP	Balance of Plant
CAPEX	Capital Expenditure
COP	Coefficient of Performance
CTC	Charge Transfer Coefficient
DH	District Heating
FLH	Full Load Hours
HHV	Higher Heating Value
HP	Heat Pump
KPI	Key Performance Indicator
LCOE	Levelised Cost of Energy
LCOH	Levelised Cost of Hydrogen
LCOHeat	Levelised Cost of Heat
OPEX	Operational Expenditure
PEM	Proton Exchange Membrane
PID	Proportional Integral Derivative
PV	Photovoltaic
RCP	Representative Concentration Pathway
SOEC	Solid Oxide Electrolyser
WACC	Weighted Average Cost of Capital

Notations

Symbol	Description
$V_{act,an}$	Activation Overvoltage at the Anode
$V_{act,ca}$	Activation Overvoltage at the Cathode
T_{amb}	Ambient Temperature
P_{an}	Anode Pressure
α_{an}	Anodic Charge Transfer Coefficient
E_{BoP}	Balance of Plant Energy Demand
P_{ca}	Cathode Pressure
α_{ca}	Cathodic Charge Transfer Coefficient
A	Cell Area
V_{cell}	Cell Voltage
$\dot{m}_{CW}$	Cooling Water Flow Rate
I	Current
t_{op}	Current Operating Hours of the PEM System
i	Current Density
V_{deg}	Degradation Overvoltage
γ_{deg}	Degradation Rate
E_{in}	Direct Input Energy to the Electrolyser
η_{DH}	Efficiency regarding District Heating Supply
η_{cool}	Efficiency with Cooling Potential
η_{el}	Electrolyser Stack Efficiency
P_{stack}	Electrolyser Stack Nominal Power
T	Electrolyser Temperature
i_0	Exchange Current Density
Q_{exch}	Exchange Heat
Q_{cool}	Extracted Cooling Heat
F	Faraday Constant
η_F	Faraday Efficiency
α_{load}	Fulfilled District Heating Demand
$FLH_{electrolyser}$	Full Load Hours of Electrolyser
R	Gas Constant
Q_{gen}	Generated Heat by Electrolysis Process
ΔG^0	Gibbs Energy Change at Standard Conditions
Q_{loss}	Heat Lost to the Ambient
R_{heat}	Heat Revenues

Symbol	Description
Q_{toDH}	Heat Supplied to District Heating Network
E_{H_2}	Hydrogen Output as Energy Value (HHV)
p_{H_2}	Hydrogen Partial Pressure
$P_{nominal,H_2}$	Hydrogen Energy Output at Nominal Power (HHV)
$T_{CW,in}$	Inlet Cooling Temperature
λ_{H_2O}	Latent Heat of Vaporisation of Liquid Water
$\dot{m}_{H_2}, \dot{m}_{H_2O}, \dot{m}_{O_2}, \dot{m}_{Vapor}$	Mass Flow Rates
i_{max}	Maximum Current Density
σ_{mem}	Membrane Material Conductivity
R_{mem}	Membrane Resistance
δ_{mem}	Membrane Thickness
λ	Membrane Water Content
$\dot{n}_{H_2}$	Molar Hydrogen Flow Rate
N_c	Number of Cells per Stack
z	Number of Electrons Involved in Reaction
V_{ohm}	Ohmic Overvoltage
T_{cool}	Outlet Temperature of Cooling Water
η_{system}	Overall System Efficiency
p_{O_2}	Oxygen Partial Pressure
a, b, c	Parameters for Faraday Efficiency Calculation
ΔH^0	Reaction Enthalpy Change
V_{rev}	Reversible Voltage
V_{rev}^0	Reversible Voltage at Certain Temperature
C	Secondary Cashflows
$C_{p,H_2}, C_{p,H_2O}, C_{p,O_2}$	Specific Heat Capacities
C_{th}	Specific Stack Thermal Capacity
R_{th}	Stack Thermal Resistance
Q_{st}	Stored Net Thermal Energy
T_{diff}	Temperature Difference of Cooling Water
Δt	Timestep of Simulation
Q_{load}	Thermal Load of the District Heating Network
V_{tn}	Thermoneutral Voltage
η_v	Voltage Efficiency
p_{H_2O}	Water Partial Pressure

Contents

1 Introduction

Worldwide, the demand for clean hydrogen is rising rapidly as it is expected to be a key factor in a sustainable future energy system. Hydrogen produced by renewable sources fulfils the role of a versatile energy carrier, which can be paramount in overcoming critical obstacles on the way toward a climate-neutral energy infrastructure. It has the potential to contribute significantly to the decarbonisation of multiple sectors (e.g. long-range transport or chemical and metallurgical industries), where the reduction of greenhouse gas emissions is particularly challenging. [1–4]
Additionally, producing hydrogen with electricity from renewables sources, especially during times of abundance, provides a solution to handling the volatile nature of wind and solar energy and can balance out peak loads. Therefore, this technology simultaneously aids the transition to clean renewable electricity production and potentially offers an option for long-term energy storage, even across seasons. [2, 5]

Consequently, developing and increasing the production of green hydrogen has received widespread interest across the globe and is a priority for the European Union. Aiming for the production of 10 million tons of H_2 by 2030 [6], substantial investments and projects are vital to achieve this goal. As far as Austria is concerned, 1 GW of electrolyser capacity are targeted to be installed by 2030 [7] and a supporting infrastructure for hydrogen is to be implemented. Due to these ambitious plans to increase hydrogen production capacity, there is a large interest in scaling up hydrogen production. [6–10]
Another key challenge for the extensive integration of green hydrogen is its economic competitiveness, since the production cost of renewable hydrogen currently remains higher than the cost of more conventional methods. Closing this gap is therefore paramount in extending the use of green hydrogen and replacing non-sustainable production technologies. [4, 8]

Electrolysis is the process of using electricity to separate water into hydrogen and oxygen. A range of technologies are available for this purpose, with alkaline and proton exchange membrane (PEM) electrolysis among the most mature and well-known; the latter is especially suited for balancing intermittent renewable energy as it provides a rapid dynamic response. The efficiency of these low-temperature methods

is however limited and currently ranges roughly from 65-85 % [11–14], when considering the higher heating value (HHV) of hydrogen. As a result, a non-negligible part of the input energy is lost as a by-product in the form of heat. As electrolyser capacities grow and more larger projects are planned, a detailed look into waste heat recovery and its link to potential efficiency improvement of hydrogen production is highly valuable. One possibility to repurpose an electrolyser's excess heat is supplying a local district heating network with the surplus thermal energy. Approaches like this could unlock additional efficiency gains in large-scale hydrogen production and be important measures for a climate-neutral energy network. [4, 10, 15–18]

1.1 Background

1.1.1 Hydrogen Production

Hydrogen in large amounts is not directly available on our planet, however different technologies exist to generate it from various raw materials. Some are more climate-neutral than others, and a colour-coded system has been introduced to differentiate between methods of production. Currently, about 95 % of the total hydrogen is based on fossil fuels. The related processes are called steam methane reforming or coal gasification, both having a considerable negative impact on CO_2 emissions and produced hydrogen is referred to as grey. An improvement in terms of sustainability is blue hydrogen, where carbon capture and storage technology is additionally applied to create a net-zero carbon balance. Green hydrogen, which is the focus of this thesis, classifies production processes utilising renewable sources to generate the molecule. Therefore, it is non-emitting and the most desirable option, which usually translates to hydrogen production via electrolysis. In recent years, other colour codes have been introduced as well to represent additional methods of hydrogen production, for instance pink is associated with hydrogen manufactured utilising nuclear energy. However, the ones mentioned above are considered the most relevant. [19–21]

Globally, hydrogen demand has risen to 97 Mt in 2023 according to the *IEA* [4], with the majority of this demand covered by fossil-based ("grey") hydrogen. Low-emission hydrogen or green hydrogen therefore only covers a minor part of total production, with numbers ranging from approximately 1 % to 5 % [4, 18, 19, 22, 23]. As touched upon before, this phenomenon is closely related to the considerably high green hydrogen production costs, which are linked to capital expenditures (CAPEX) of electrolysis. In 2023, as per the *European Hydrogen Observatory* [24], the production costs in Europe spanned roughly from 9-4 €/kg for sustainable hydrogen compared to grey hydrogen, which has a lower cost of about 3.5 €/kg.

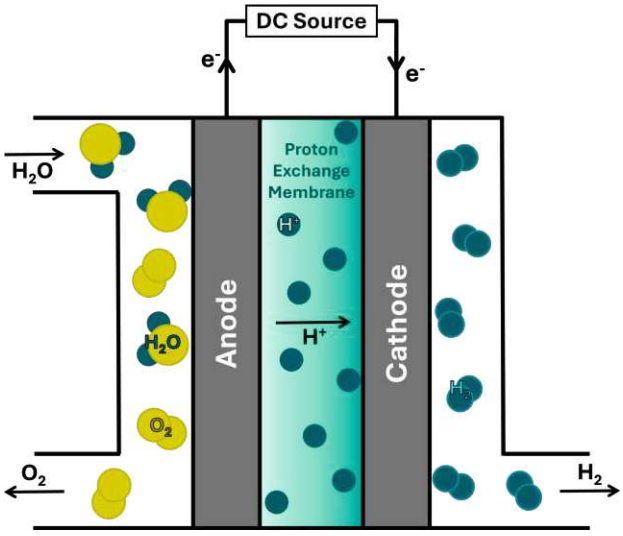

Figure 1.1: Basic structure of a PEM electrolyser cell.
Adapted from [26] under CC Attribution 4.0 International License (https://creativecommons.org/licenses/by/4.0/)

Other sources indicated in recent years that globally green hydrogen needs to drift towards 1.5-2€/kg to become cost competitive, as grey hydrogen costs typically range from 0.7-2.5€/kg [4, 20, 21, 23, 25].

1.1.2 Proton Exchange Membrane Electrolysis

In the context of water electrolysis three main technologies have emerged: Alkaline (AEL), proton exchange membrane (PEM) and solid oxide electrolysis (SOEC). The two former ones are so-called low-temperature technologies, while the SOEC operates in a significantly higher temperature range. Additionally, these methods have varied levels of maturity, with AEL being the most established one and SOEC still in development. The PEM technology is considered one of the most promising for future applications. This particular electrolyser has quite a few advantages, compared to the well-developed AEL, as it offers a fast cold start-up time, a rapid dynamic response, a large range of operation as well as a high current density and output pressure. [3, 15, 18, 26]

The basic working principle of a PEM electrolyser is the same as for all water electrolysers: Electrical energy is used to electrochemically split water (H_2O) into hydrogen (H_2) and oxygen (O_2). A PEM cell, specifically, can be divided into three main components: anode, cathode and a proton conducting membrane (see Figure 1.1). At the anode purified water is separated into protons, electrons and O_2. Subsequent to this oxygen evolution reaction 1.1, protons are traversing the membrane to the cathode, while the electrons get there via a connected power source.

At the cathode, the hydrogen evolution reaction 1.2 happens, which results in the generation of H_2 [27].

$$Anode: \qquad H_2O \longrightarrow 2\,H^+ + \frac{1}{2}\,O_2 + 2\,e^- \tag{1.1}$$

$$Cathode: \qquad 2\,H^+ + 2\,e^- \longrightarrow H_2 \tag{1.2}$$

Consequently, the total water electrolysis reaction is the aforementioned:

$$H_2O \longrightarrow H_2 + \frac{1}{2}\,O_2 \tag{1.3}$$

The water splitting reaction starts to occur within the electrolyser once the applied DC voltage is higher than the thermodynamic reversible voltage V_{rev} at the existing conditions - in an ideal situation without losses, where the necessary thermal energy is otherwise available. The reversible potential is correlated to the free Gibbs energy of the process, representing the electrical demand, and in combination with the Faraday constant F and the number of electrons z involved in the reaction, it can be evaluated at standard conditions (1 atm; 298.15 K) as follows:

$$V_{rev}^0 = \frac{\Delta G^0}{zF} = 1.23\,V \tag{1.4}$$

Since no external thermal energy is supplied to low-temperature electrolysers, the total required energy (this equals the reaction enthalpy change ΔH^0), consisting of a thermal and electrical part, needs to be supplied via the electrical input. The necessary potential is called the thermoneutral voltage V_{tn}, which can be calculated analogous to the reversible voltage, merely with ΔH^0. It has the value of 1.482 V and, in contrast to the reversible potential, it remains relatively constant with varied temperature and pressure. [28, 29]

As stated previously, PEM electrolysis has relatively low operating temperatures, typically around 50-80 °C [14, 30]. In comparison, the operating pressure is rather high, with commercial electrolysers generally functioning at an hydrogen outlet pressure of roughly 30-40 bar [31]. Furthermore, a PEM system has the disadvantage, compared to AEL, that noble and therefore expensive as well as rare materials are required for the electrodes, specifically for the electrocatalyst layers, in order to reach a sufficient level of activity. Currently, iridium-based catalysts are commonly used at the anode, while platinum is usually implemented at the cathode. Together, the electrocatalyst layers account for approximately 8 % of stack electrolyser costs [26, 27, 32]. While this can affect the large-scale deployment of the technology,

an arguably bigger issue presents the scarcity of these materials. In particular, the future supply of iridium could be a bottleneck as PEM electrolyser capacities grow significantly worldwide. Consequently, substantial research is being done to replace these materials or minimise their usage within the catalyst layers. [26, 27, 33, 34]

1.1.3 District Heating Networks and Heat Pumps

District Heating (DH) networks have the purpose of distributing heat using steam or water to areas of need (e.g. households or office buildings). Such networks are largely found in densely populated areas due to the shorter distances, however also smaller towns of a few thousand inhabitants employ local networks [35]. Since their implementation, several generations of heating networks have been introduced using a variety of heat carriers at different temperatures. Generally it can be said that the newer networks are operating with lower temperatures, ranging from supply temperatures of significantly above 100 °C for the first generation to below 30 °C for the fifth generation ("ultra-low"). [17, 36–38]
In Austria, the majority of district heating networks can be defined as older generations, especially in rural areas, and therefore require minimum feed-in temperatures of roughly 90-110 °C, at the very least during winter periods [39, 40]. Additionally, hygienic regulations for domestic hot water are in place, which demand a minimum temperature of 65 °C [36]. Consequently, comparing DH and PEM temperature levels, either electrolysis waste heat is supplied directly to a newer low-temperature district heating network, or a heat pump is imperative to supply excess heat to installed heating networks in Austria.

The integration of heat pumps (HP) enables the effective utilisation of various (waste) heat sources to be a supply source for district heating networks [39] or to cover other industrial heat demands within a constrained temperature range. Therefore, the adoption of heat pump technology holds significant potential to aid in the decarbonisation of the heating sector. This technology provides a very efficient way to elevate the temperature level of a heat source driven by electrical energy. With the enormous increase in renewable electricity generation, a HP therefore offers a sustainable solution. The effectiveness of a HP is determined by the coefficient of performance (COP), which is defined as the ratio between the thermal energy output and the input of electrical energy. The effective COP can further be defined as the product between an ideal COP, dependent on the in- and output temperatures, and an efficiency term, which correlates to losses within the practical process. Common values for the COP are found to be within 2-5 [30, 41–43] depending on the exact application. [42, 44]

1.2 Purpose and Scientific Questions

This thesis aims to perform a techno-economic analysis of a potential future renewable energy system operated between 2030-2050 centered around a large-scale PEM electrolyser. It is situated in eastern Austria and in the range of hundreds of MW. The system includes renewable energy sources — specifically wind and photovoltaic (PV) — that supply electricity to the electrolyser, with their capacity varied for impact assessment. To ensure a continuous production, a grid supply connection is provided as well. The hydrogen produced is then injected into a hydrogen pipeline, linking the rural production site with Vienna. Furthermore, this study explores the potential of redirecting the waste heat generated in the process to supply a local district heating network. Key performance indicators (KPIs), technical and economic, are examined, focusing on efficiency and the Levelised Cost of Hydrogen (LCOH) and Heat (LCOHeat), as well as how these metrics depend on different system configurations. As such, this work makes an attempt to answer the following scientific questions:

- What is the potential of a large-scale PEM electrolysis plant mainly powered by renewables to produce hydrogen and simultaneously provide heat for local district heating networks?
- What is the theoretical attainable stack efficiency enhancement considering recycling of excess heat?
- How is the LCOH impacted by the capital costs of the electrolysis system?
- What is the Levelised Cost of Heat and therefore, is the heat supply itself viable?

For the purpose of this analysis, an existing, hybrid power plant simulation tool is used, for which a rather comprehensive PEM model is developed and integrated. Hereby, the primary goal is to create an instrument capable of conducting a satisfactory simulation, especially in terms of heat generation, for a techno-economic analysis while preserving simplicity and code performance to a certain degree.

1.3 Delimitations

The simulated system only consists of renewable generation, a grid connection, required converters, the electrolyser itself and a heat pump for a higher supply temperature as well as the sinks - H_2 pipeline and DH network - for hydrogen and heat. As a result, storage components are not considered. The hydrogen sink is assumed to

have seemingly "unlimited" capacity for hydrogen input and the usable heat output is supplied directly to the network at each moment specifically, provided it does not surpass the heat demand. Geographically, the hybrid power system is positioned near the local district heating network. In addition, electrolyser operation is not optimised based on fluctuating energy prices and the simple approach to assume constant electricity prices depending on the scenario is applied. Similarly, a lump tariff for selling heat is utilised to do an economic estimation. Also, although an effort was made to consistently make assumptions (e.g. for system parameters) for the intended time period (2030-2050), it was not always feasible without compromising reliability and robustness.

1.4 Structure

Following this introductory part with insight into the background, chapter 2 covers the methodology. The investigated scenarios and the simulation procedure of the techno-economic assessment are described in detail as well as the integrated model for PEM electrolysis, including limitations for both model and system. Ultimately, in chapter 3, findings are displayed and reviewed including a model validation, precise simulation analysis, KPI (Key Performance Indicator) results and an examination of cost contribution factors.

2 Methodology

2.1 System and Simulation Overview

2.1.1 System Definition and Boundaries

To perform a techno-economic analysis, the scope of the system and its simulation need to be carefully defined, as well as assumptions have to be made and justified. For this work, the targeted system is depicted in Figure 2.1. As shown, main components of the overall setup include a wind park and a PV plant as the renewable sources, a grid connection for required additional electricity, necessary converters, the PEM electrolyser, a heat pump and the energy drains for hydrogen and heat. A goal of this thesis is to evaluate the impact of renewable generation sizing with respect to the electrolyser on different KPIs. Hereby, sizes of the wind and PV park each range from 0-140 % of the electrolyser capacity during simulation. Four different electrolysers capacities are investigated, 60, 100, 200 and 300 MW, which results in a combined renewable generation from 0 to 280 MW for a 100 MW electrolyser. The AC/DC converter is designed to ensure sufficient supply for the PEM electrolyser with its nominal DC electricity load, while avoiding oversizing to minimise capital expenditures. The HP capacity is fitted to the maximum heat demand of the local district heating network. As mentioned above, the hybrid power plant as well as the DH network are located in eastern Austria, a region known for high renewable potential within the country. The simulation itself is performed from 2030 to 2050, spanning 20 years of a future energy system. This helps in adequately considering the limited lifetime of components and degradation aspects of the electrolysis system.

In relation to the additional supply of electricity from the grid, two operational strategies are defined and examined. Both scenarios target a continuous production of hydrogen and therefore, it is essential that the minimum load of the electrolyser stack is always available to avoid a shut-down of the PEM system.
In the first scenario, later referred to as "base-load", 20 % of electrolyser stack capacity is constantly supplied from the grid. This setting has the advantage that due to its non-fluctuating and predictable nature, the assumed electricity price is lower than for the alternative (for exact values see section 2.4).

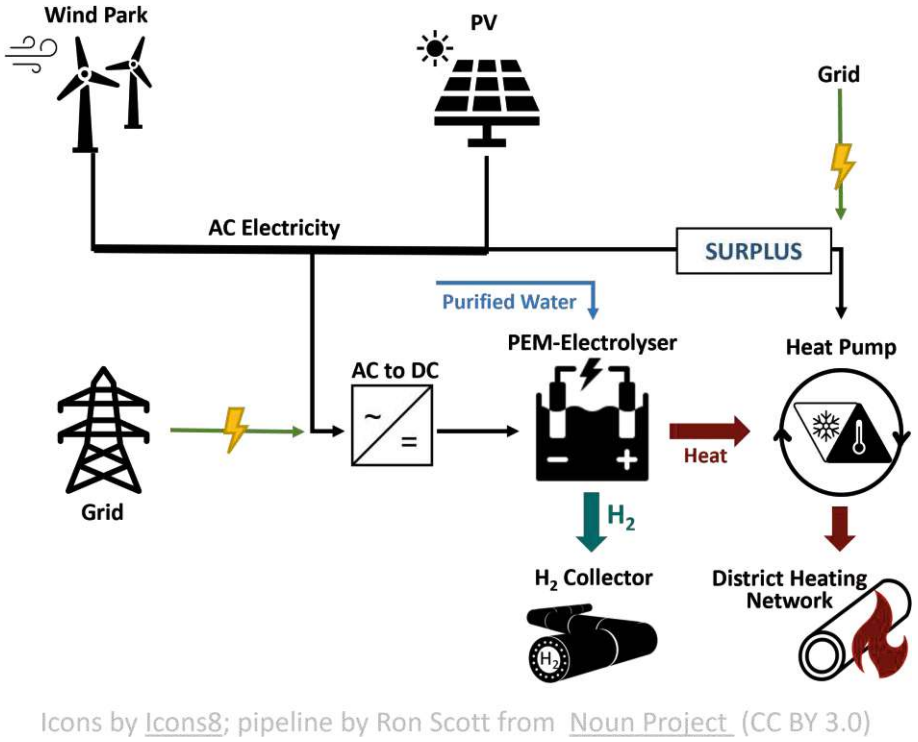

Figure 2.1: System Boundaries and Visualisation

In the second, "volatile" scenario, continuous operation of the electrolyser is also secured by ensuring a minimum of 20 % of the electrolyser stack nominal load as power input. However, in comparison, electricity is only externally supplied if the combined power input of renewables does not reach the aforementioned value. During these periods, the electricity shortfall — i.e. the difference between the renewable generation and the 20 % minimum requirement — is purchased from the grid at a constant, relatively high price. Consequently, this second scenario represents the intermittent nature of the renewables and is therefore more costly per energy unit. Moreover, in each of the presented scenarios, the electricity demand of the integrated heat pump is largely fulfilled by the grid. However, during simulating steps of surplus renewable electricity generation in regards to the nominal electrolyser capacity, the excess energy is supplied to the HP. Ultimately, both operational strategies assume the electricity sourced from the grid to be climate-neutral, maintaining the context of green hydrogen production.

The local district heating system within the analysis is chosen based on its proximity to the location of the hybrid power plant. Due to the location in a rural region, the total heat demand is rather small and peaks at around 0.65 MW (for sources see section 2.1.2). During the summer the heat demand is considerably lower as outside temperatures are higher.

The core electrolyser is made up of so-called stacks and cells. The smallest unit is a cell, its structure is described in section 1.1.2, and a certain number of these are serially connected to form a stack, a modular unit, which is utilised to generate the desired nominal power of the electrolyser by electrically connecting them in parallel. However, the complete electrolyser component also includes auxiliary equipment indispensable for operation (e.g. pumps, water purification system, etc.). This includes infrastructure for cooling, which entails a heat exchanger. Also referred to as Balance of Plant (BoP) [45–47], the related electricity demand of these utilities is defined as a constant percentage of the nominal electrolyser stack power.

The simulation software requires a range of input parameters before a simulation run can be started. Initially all components (e.g. PV, wind, electrolyser) and their capacities have to be selected and furthermore, relevant input assumptions and parameters (listed in Table 2.1) for the newly implemented model need to be chosen.

Parameter	Unit	Value	Source
Targeted Operation Temperature	°C	80	[18, 48, 49]
Cathode Pressure P_{ca}	bar	30	[31, 50–53]
Anode Pressure P_{an}	bar	2	[12, 49, 54]
Number of Cells per Stack N_c	-	310	[12, 53]
Stack Nominal Power P_{stack}	MW	10	[12]
Cell Area A	m^2	0.5	[12, 53]
Membrane Thickness δ_{mem}	μm	80	[53, 55]
Minimum Load	%	10	[30, 56]
Stack Lifetime	h	80 000	[14, 52]
Balance of Plant	%	5	[57, 58]
Degradation Rate γ_{deg}	μV/h	3.8×10^{-6}	[14, 59]
Specific Stack Thermal Capacity C_{th}	J/(kW K)	3000	[54]
Stack Thermal Resistance R_{th}	K/W	0.09	[54]

Table 2.1: Characteristics of PEM Electrolyser System

2.1.2 Data Collection and Software Usage

In addition to the parameters mentioned above, which are largely based on literature, various input profiles are crucial for performing the simulation. These include profiles for wind and PV power generation as well as the heat demand profile of the DH network. The simulation operates in timesteps of 15 min for the duration of 20 years, resulting in a total of 701 277 steps. The renewables profiles are based on the

SECURES-Met dataset [60], which is a meteorological dataset for Europe with a relatively high spatial and temporal resolution. It considers climate change projections for the future and for this work a low emission scenario is selected that satisfies the 2 °C criteria of the UNFCCC Paris Agreement 2015, RCP 4.5 [61]. Further, the district heating demand profile is derived from the European Hotmaps Project [62]. Hereby, for scaling purposes, the annual demand is determined using data from the Austrian Heat Map [35].

The techno-economic assessment is conducted using a previously developed simulation framework, with its core simulation code implemented in the programming language *Julia*. However, essential processing steps before the main technical simulation (e.g. handling data input formats) as well as post-processing tasks (e.g. economic assessments and plotting) are executed using *Python*.

2.2 Modelling PEM Electrolysis

The implemented electrolyser model on a cell and stack level targets an adequately accurate calculation of significant electrolysis outputs like hydrogen and useable heat. It is divided in two main parts: the electrochemical and the thermal model.

2.2.1 Electrochemical Model

Within the electrochemical submodel of the overall PEM model, the cell voltage, stack efficiency and hydrogen output are determined based on various parameters inputs, stack characteristics as well as temperature and current density at the present timestep. Important sources are [28] and [50], with the exception of degradation.

In an ideal electrolysis process the reversible voltage V_{rev} would be sufficient for the reaction to occur. However, a realistic PEM electrolyser suffers various losses that affect the required electrical potential for the electrochemical process. Activation overvoltages ($V_{act,ca}, V_{act,an}$) are crucial to aid kinetics and start reactions at the electrodes. To counteract resistances arising within the cell due to electron and proton flows, an ohmic overpotential V_{ohm} is introduced. Ultimately, a PEM cell degrades over time, which also decreases the voltage. Consequently, a degradation overvoltage V_{deg} is essential to compensate for this voltage drop. The cell voltage is therefore calculated as a sum of all voltage factors described above, see equation 2.1. It does not consider a diffusion overpotential, as it does not typically influence the

cell voltage during electrolyser operation at ordinary current densities [28, 48, 50].

$$V_{cell} = V_{rev} + V_{act,an} + V_{act,ca} + V_{ohm} + V_{deg} \tag{2.1}$$

Reversible Voltage

As stated in section 1.1.2, the reversible potential V_{rev} (also called open circuit voltage) is dependent on both operational temperature and pressure. To determine the correct reversible voltage at current conditions, the Nernst Equation (2.2) is applied first within the model [49, 50, 63]:

$$V_{rev} = V_{rev}^{0} + \frac{RT}{zF} ln \left(\frac{p_{H_2} \sqrt{p_{O_2}}}{p_{H_2O}} \right) \tag{2.2}$$

The first mathematical term V_{rev}^{0} represents the reversible potential at standard pressure. Dependent on the temperature T, it is estimated with the following empirical expression [49, 50]:

$$V_{rev}^{0} = 1.229 - 0.9 \times 10^{-3} \, (T - 298.0) \tag{2.3}$$

Secondly, the influence of pressure on V_{rev} needs to be considered. In this term R, F and z are the gas constant, faraday constant and the number of electrons transferred in the reaction, respectively. Moreover, the variables p_X signify the partial pressures for the involved molecules H_2, O_2 and H_2O and are determined as follows [50]:

$$p_{H_2} = P_{ca} - p_{H_2O} \quad | \quad p_{O_2} = P_{an} - p_{H_2O}. \tag{2.4}$$

$$p_{H_2O}(T) = 6.1078 \times 10^{-3} \cdot \exp \left(\frac{17.2694 \cdot (T - 273.15)}{T - 34.85} \right) \tag{2.5}$$

As portrayed, the partial pressures of hydrogen and oxygen are calculated via Dalton's law using the electrode outlet pressures P_{ca}, P_{an} (see equations 2.4), while an empirical formula (2.5) is applied for the pressure of water. For this approach several assumptions are necessary, which are described closely in [50] and [64].

Activation Overvoltage

The activation overvoltage V_{act} is determined using a simplified expression (equation 2.6) derived from the Butler-Volmer equation for both cathode and anode. It includes a logarithmic dependency on the fraction of current density i and exchange current density i_0, whereas α represents the charge transfer coefficient (CTC) [3,

28, 63, 65, 66].

$$V_{act} = \frac{RT}{z\alpha F} \ln\left(\frac{i}{i_0}\right) \quad and \quad i = \frac{I}{A} \tag{2.6}$$

Considering the significant variability in the reported values of i_0 and α for each electrode in literature, a definitive selection of these parameters remains challenging [28, 48, 49]. However, there is a tendency to choose 10^{-7} and $10^{-3}\,\mathrm{A/cm^2}$ for a Pt-Ir Anode and a Pt Cathode [50], which is applied during this work as well. The anodic (α_{an}) and cathodic (α_{ca}) charge transfer coefficient, are kinetic values that represent the portion of potential energy, which raises the reaction rate at the respective electrolyte-electrode interface [48, 50]. In literature, α is commonly treated to be a symmetry factor of 0.5, correlating to a perfectly (anti-)symmetric $i - V_{act}$ curve. It is generally understood that the charge transfer coefficient tends to differ from this exact value in practical applications, and therefore various values are reported across a relatively wide range [28, 48, 50, 63, 64]. Particularly the anodic CTC is varied considerably and a few literature sources report typical values of α_{an} to be 2 [49, 67], additionally it is usually higher than the cathodic equivalent due to a larger overpotential at the anode [63]. Consequently, α_{an} is intentionally kept variable to a certain extent, allowing for fitting of the polarisation curve during the model validation process.

Ohmic Overvoltage

Cell voltage drops due to the proton flow through the PEM membrane (ionic losses) and electron flow within the electrodes (electronic losses) result in the necessity of the ohmic overvoltage V_{ohm}. The majority of the ohmic resistance is caused by the protonic movement, therefore making it the dominant factor. Hence it is assumed to be sufficient to only model this loss within the electrolyte, as done in a range of other works before [28, 47, 50]. The calculation of the ohmic overpotential follows the conventional Ohm's law (equation 2.7), where the resistance of the membrane R_{mem} is given by the fraction of membrane thickness δ_{mem} and material conductivity σ_{mem}.

$$V_{ohm} = R_{mem} \cdot i \quad | \quad R_{mem} = \frac{\delta_{mem}}{\sigma_{mem}} \tag{2.7}$$

The latter is determined empirically below (equation 2.8) based on the water content λ within the membrane [28, 50, 67]. According to [50], [68] and [49] λ has a value of approximately 22, when the membrane is subjected to liquid water, as is the case in PEM electrolysis. However, in this work, an empircial expression (2.9) is applied for the determination of the parameter, following Hernández-Gómez et al.'s

approach [3].

$$\sigma_{mem} = (0.005139 \cdot \lambda - 0.00326) \cdot \exp\left(1268 \cdot \left(\frac{1}{303} - \frac{1}{T}\right)\right) \tag{2.8}$$

$$\lambda = 0.08533 \cdot T - 6.77632 \tag{2.9}$$

Degradation

Considering the duration of the executed simulation, it encompasses the entire lifecycle of a PEM electrolyser. Therefore, it is crucial to account for the degradation by modelling the correlated voltage overpotential V_{deg}. For this, a degradation rate γ_{deg}, accounting for the hourly voltage drop, is multiplied by the total hours of operation t_{op} up until that point in the simulation [52, 59] - see equation 2.10. Moreover, since the degradation rate is related to the nominal load of the electrolyser [14] and dependent on the current density [69], the overpotential has to be scaled accordingly, which is done by building the fraction of i and the maximum current density i_{max} at the beginning of operation.

$$V_{deg} = \gamma_{deg} \cdot t_{op} \cdot \frac{i}{i_{max}} \tag{2.10}$$

Efficiency and Hydrogen Output

The applied formulas for efficiencies of the PEM stack are listed in equations 2.11 and 2.12. The Faraday efficiency η_F of an electrolyser cell quantifies the ratio between the actual hydrogen output and the theoretical maximum. Losses linked to this efficiency arise from parasitic currents, which are more significant at lower current densities, and an empirical model is applied in this context [70]. Furthermore, electrical losses are accounted for by the voltage efficiency η_v, which is largely dependent on the cell voltage. The overall efficiency of the electrolyser stack η_{el}, excluding auxiliary losses, is determined by the product of these two efficiencies [3, 27].

$$\eta_F = a\left(\frac{i}{A}\right)^b + c \quad | \quad a = -0.0034 \cdot P_{ca} - 0.001711,\ b = -1,\ c = 1 \tag{2.11}$$

$$\eta_v = \frac{V_{tn}}{V_{cell}} \tag{2.12}$$

Faraday's law indicates that the amount of H_2 produced at the electrode is directly proportional to the current passing through the electrolyser. As a result, the molar hydrogen flow rate $\dot{n}_{H_2}$ generated per stack can be expressed as shown in equation 2.13 below [3, 50, 63, 67]. Here, N_c is the number of serially connected cells within

the stack, while I represents the current.

$$\dot{n}_{H_2} = \eta_F \cdot \frac{N_c I}{zF} \tag{2.13}$$

2.2.2 Thermal Model

A model of thermal processes in the electrolyser is crucial for evaluating the useable heat output of the component. Within this submodel the temperature of both the electrolyser and the extracted cooling water are calculated as well as various factors of thermal energy, focusing on the thermal energy output that can be utilised for the connected district heating network.
A lumped thermal capacitance model is applied, this means the electrolyser stack is considered as one thermal unit with homogeneous temperature. This type, developed by Ulleberg [29], is frequently used in literature [47] and vital sources for the implemented model include the following: [38, 50, 54, 66, 69, 71]. The resulting heat balance is listed below in equation 2.14.

$$\dot{Q}_{st} = C_{th} P_{stack} \frac{dT}{dt} = \dot{Q}_{gen} - \dot{Q}_{loss} - \dot{Q}_{exch} - \dot{Q}_{cool} \tag{2.14}$$

Here, Q_{st} represents the net energy stored in the electrolyser after each simulation step and depends on several thermal energy factors. The electrochemical reaction of a PEM electrolyser generates heat Q_{gen} as it typically operates above the thermoneutral voltage [66]. Therefore, a cooling mechanism is commonly required, correlating to the extracted heat Q_{cool}. The heat loss to the ambient Q_{loss} as well as Q_{exch} are ultimately forms of heat that are lost. The latter depicting thermal energy transferred to sensible and latent heat [71]. The described variables are determined as follows:

$$\dot{Q}_{gen} = V_{cell} \cdot N_c \cdot I \cdot (1 - \eta_v) \tag{2.15}$$

$$\dot{Q}_{loss} = \frac{T - T_{amb}}{R_{th}} \tag{2.16}$$

$$\begin{aligned} \dot{Q}_{exch} = {} & \dot{m}_{H_2} C_{p,H_2} (T - T_{amb}) + \dot{m}_{O_2} C_{p,O_2} (T - T_{amb}) \\ & + \dot{m}_{H_2O} C_{p,H_2O} (T - T_{amb}) + \dot{m}_{Vapour} \lambda_{H_2O} \end{aligned} \tag{2.17}$$

To estimate Q_{exch}, sufficient knowledge of all mass flows inside the electrolyser is needed. Within equation 2.17, $\dot{m}_X$ represents the flow rates of involved gases - H_2, O_2 - and liquid H_2O as well as water vapour. Additionally, $C_{p,X}$ depicts the respective specific heat capacity, while λ_{H_2O} symbolises the latent heat required to vaporise liquid water. Calculation of all mass flows can be achieved by knowing the total mass balance [71] and applying the stoichiometry of the electrolysis reaction as well as Faraday's law [3, 49, 50, 69, 71].

Cooling Mechanism

The implementation of the cooling mechanism for the electrolyser is centered around the estimation of $\dot{Q}_{cool}$. At the start of operation the temperature of the PEM system is equal to the ambient temperature (set at 22 °C) since no additional heating equipment is considered. Therefore, initially the generated heat from the electrochemical reaction is utilised to heat up the electrolyser. Once the target electrolyser temperature is reached, cooling starts up. The linked extraction of thermal energy is calculated as expressed below [38, 51, 69, 71]:

$$\dot{Q}_{cool} = \dot{m}_{CW} C_{p,H_2O} T_{diff} \tag{2.18}$$

T_{diff}, defined as an input parameter within this model, represents the difference between the in- and outlet temperature of cooling water. This aids a flexible application of the model for potential future analyses concerning heat utilisations. The mass flow of the cooling liquid $\dot{m}_{CW}$ is utilised as the controlled variable in a simple PID-Controller. This algorithm, similarly implemented in [50, 68, 72, 73], adjusts the selected variable and therefore the cooling effect to maintain the system at the desired operational temperature, striving to ensure stable production by minimising deviations from the set point. However, once the current electrolyser temperature is within a certain interval (±0.25 °C) from the targeted value, the extracted cooling heat is directly calculated by setting equation 2.14 to zero as long as the electrolyser is operating to optimise performance.

$$T(t) = T(t - \Delta t) + \frac{\Delta t}{C_{th} P_{stack}} Q_{st} \quad | \quad T_{cool} = T_{CW,in} + T_{diff} \tag{2.19}$$

Following that, the resulting electrolyser temperature as well as the cooling output temperature can be calculated (equation 2.19 above). To estimate the temperature within the PEM system a relatively simple quasi steady-state model, proposed by Ulleberg [29], has been applied. The assumption is to have constant generation and transfer of thermal energy within each timestep.

2.3 Technical Analysis

2.3.1 Simulation Procedure

The specific design and operational flow of the simulation framework, applied in the present work for conducting the techno-economic analysis, is portrayed in Figure 2.2. First essential input data is provided, followed by the realisation of the overall system simulation, as depicted previously in Figure 2.1. Finally, the analysis

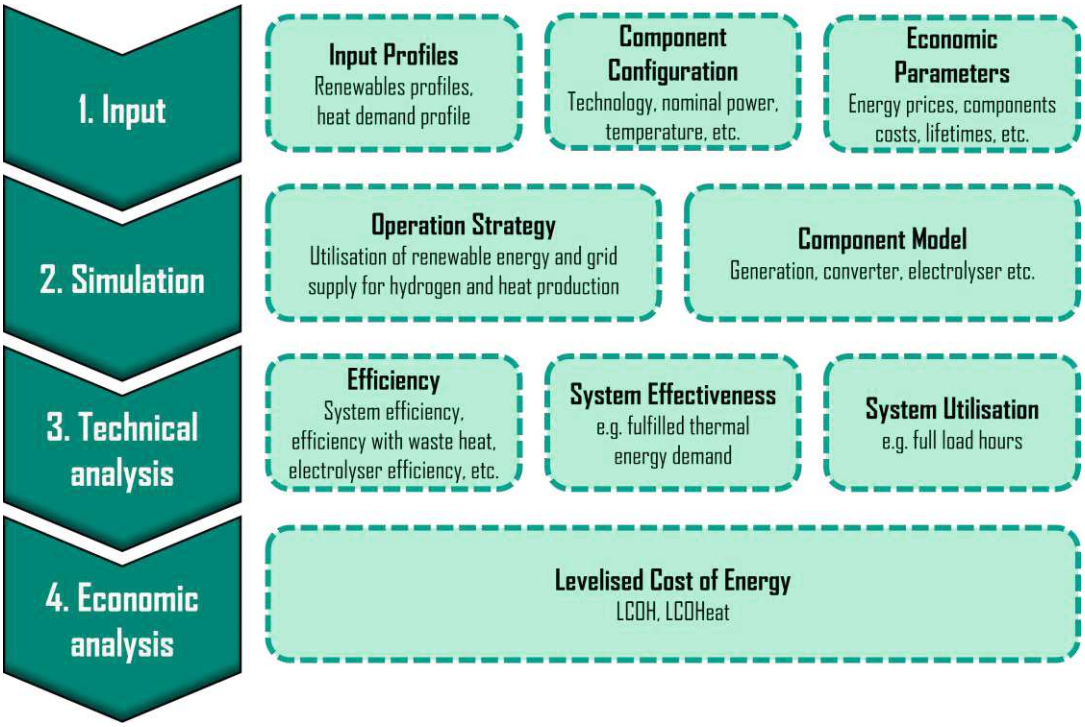

Figure 2.2: Outline of Simulation Framework

focuses on assessing the system's technical and economic performance by evaluating key performance indicators (KPIs) and interpreting the results. The simulation methodology resembles the approach outlined in [38].

The simulation tool is largely split into components, each of which characterises a particular part of the overall system to be simulated. Electricity inputs (e.g. wind or PV energy) represent a generational component, providing the available electricity (in units of power). An AC/DC Converter is essential for providing DC electricity to the electrolyser. The latter defines the largest and arguably, in this simulation, the most complex component, based on the electrolysis model that is described above (section 2.2) and implemented within the framework in *Julia*. However, to enable the execution of the simulation, electrical power must be converted into current and voltage, as the former is a required input for the electrolyser model. To address this, a "design" module is integrated, featuring a solving function to estimate the stack voltage and calculate the appropriate current input prior to the actual model calculations. Additionally, the electrolyser implementation accounts for the fact that the model represents only a single stack, with scaling applied to embody the complete system. Ultimately, the heat pump required for elevating the temperature level of the waste heat is its own entity. The hydrogen pipeline, known as "H_2 collector", is not part of the technical assessment and is therefore only considered for its economic impact and as a hydrogen sink. Similarly, the DH network is only characterised by its heat demand profile, which is an input for the system.

Heat Pump and Integration into District Heating Network

As implied before in section 1.1.3, a HP is necessary for supplying electrolysis excess heat to the rural district heating network, considering the temperature level of the PEM technology. Specifically, within this analysis the output cooling temperature is set to 65 °C. To assess the feasibility of providing waste heat, it is essential to estimate the electrical demand of the integrated water-water heat pump, which is done by assuming an average COP of 3.66. This corresponds to raising the temperature from 65 °C to 110 °C, with a practical efficiency of 43 % [74]. It therefore represents a conservative scenario as it assumes a high temperature demand of the DH network year-round. The thermal energy demand of the DH network serves as the basis for the thermal energy dataset, which is then used to ultimately calculate the electrical demand of the heat pump, majorly supplied by the grid (see section 2.1.1). Within the simulation, the waste heat potential of the electrolyser Q_{cool} is compared to the DH demand at each timestep. Consequently, if cooling would be deactivated, no heat could be supplied to the network. However, as the operating strategy (closely defined in section 2.1.1) results in a continuous operation of the electrolyser, excess thermal energy can constantly act as a supply source.

2.3.2 Technical KPIs

To assess the system's technical performance, various key performance indicators (KPIs) are defined and computed. Each KPI is calculated for every configuration of all varied capacities within the system to create a comprehensive analysis. All energy values in the subsequent equations represent the total annual energy generated, averaged over the simulation timespan.

$$FLH_{electrolyser} = \frac{E_{H_2}}{P_{nominal,H_2}} \tag{2.20}$$

$$\eta_{system} = \frac{E_{H_2}}{E_{in} + E_{BoP}} \tag{2.21}$$

$$\eta_{cool} = \frac{E_{H_2} + Q_{cool}}{E_{in}} \quad | \quad \eta_{DH} = \frac{E_{H_2} + Q_{toDH}}{E_{in}} \tag{2.22}$$

$$\alpha_{load} = \frac{Q_{toDH}}{Q_{load}} \tag{2.23}$$

The KPIs depicted (similarly implemented in [38]) include the full load hours (FLH) of the electrolyser (2.20), as a fraction of the nominal hydrogen production rate $P_{nominal,H_2}$ and the hydrogen produced E_{H_2}, expressed in power (correlated to the HHV). The system efficiency η_{system} of the complete electrolysis component is also

calculated, taking into account the required balance of the plant E_{BoP}. E_{in} signifies the electrical DC input into the electrolysis stack system itself. Considering the objective of this thesis, efficiencies regarding the thermal energy output of the PEM electrolyser are listed as well. η_{cool} is the theoretical value of enhanced stack efficiency, if the total amount of useable excess heat could be utilised. Comparatively, η_{DH} shows the improved efficiency when considering the heat Q_{toDH} actually supplied to the local district heating network. Finally, in equation 2.23 the value α_{load} is estimated, which represents the share of heat demand by the DH network that can be fulfilled by the electrolyser waste heat.

2.4 Economic Evaluation

The economic assessment within the present work is focused on various forms of the Levelised Cost of Energy (LCOE). To perform the calculations, it is essential to define the capital expenditures (CAPEX) and operational expenditures (OPEX) for each component. The used CAPEX values for the relevant components are provided in Table 2.2. Setting a reliable CAPEX value for the PEM system is quite challenging, as a broad range of costs are reported in literature. Future projections for 2030 and beyond suggest optimistic cost reductions for PEM electrolyser stack components, with estimates ranging from approximately 250 to 400 €/kW, particularly for large-scale installations [32, 53, 57, 75, 76]. In contrast, current electrolyser system prices are reported to be between 800-1000 €/kW, based on various sources [32, 52, 57–59, 77]. However, insights from industry experts indicate that total capital expenditures can rise significantly, reaching around 2000 €/kW or more [78]. Furthermore, it is assumed that operating expenditures amount to 2 % of the corresponding CAPEX values [30, 79]. An exception is made for the PEM system, for which the OPEX represents 3 % of capital costs in the present work due to literature reporting values between 1-5 % [14, 52, 59, 80–82], excluding supplied electricity costs.

Component	**Value** [€/kW]	**Source**
PEM Electrolyser System	900	[32, 57, 59, 77]
AC/DC Converter	150	[83, 84]
Photovoltaic Plant	340	[79]
Wind Park	1075	[79]
Heat Exchanger	90	[85]
Heat Pump	600	[30, 86]

Table 2.2: Relevant CAPEX values

The LCOE reflects the average cost of producing energy over the system's lifetime and therefore represents the minimum price needed for economic viability. As shown in equation 2.24 [38, 59], the calculation requires CAPEX, OPEX and the weighted average cost of capital (WACC), estimated at 6 % [82]. C_t additionally signifies other types of cashflows like electricity costs or grid charges. The latter are implemented according to current values based on the grid voltage level and the region in Austria [87]. Hereby solely the energy and load rates are considered. Regarding electricity supplied from the grid, the operational strategy defines the assumed constant electricity rate (described in section 2.1.1). For the *base-load* scenario, a price of 80 €/MWh is set, while within the *volatile* strategy a value of 120 €/MWh is applied [88].

$$LCOE = \frac{\sum \frac{CAPEX_t + OPEX_t + C_t - R_{heat,t}}{(1+wacc)^t}}{\sum \frac{E_t}{(1+wacc)^t}} \tag{2.24}$$

The Levelised Cost of Hydrogen evaluates the competitiveness of the system's hydrogen price relative to other production methods. Factors that contribute to the LCOH are capital and operational costs of renewables, electrolyser system and converter as well as electricity costs and grid charges. An additional factor considered in this work is a lump feed-in tariff for the H_2 collector, defined at 0.013 €/kg [88]. First, the hydrogen costs are determined without accounting for revenues from supplying heat to the DH network ($R_{heat} = 0$). Second, the effect of heat sales on hydrogen pricing is examined by defining the potential profits from providing heat. Based on literature, a pessimistic scenario at 25 €/MWh and an optimistic scenario at 40 €/MWh are considered [38, 89, 90].
To assess the economic viability of selling the produced thermal energy at the specified prices, calculating the Levelised Cost of Heat (LCOHeat) is essential. The assumption is, that the electrolyser is primarily designed to produce hydrogen. Therefore, only costs directly associated with the heat supply are considered in the calculation of this particular KPI. This includes heat exchanger and heat pump expenditures and electricity costs of the HP as well as grid connection charges. Formula 2.24 is utilised without considering the term R_{heat}.

2.5 Model and System Limitations

In the simulation framework, the AC/DC converter is the only component directly linked to the electrolyser that is simulated independently. Other electrolysis auxiliary systems, such as the water deioniser or pumps, part of the BoP, are simplified

by estimating their energy consumption as a fixed percentage of the electrolyser's electricity input. This approach reduces complexity while ensuring that key operations of the system are accurately represented.

The simulation spans a 20-year timespan, during which system components are repurchased at the end of their operational lifetime as needed. For the LCOE calculation, these components are assumed to be resold at the end of the simulation period at a reduced price, recouping a portion of the initial CAPEX. The residual value and selling price of each component are determined proportionally, based on the ratio of its elapsed operational time to its total expected lifetime.

Regarding the electrolyser model itself, several simplifications have been applied throughout the model. For instance, experimental data for the specific utilised PEM stack was unavailable, so parameters are otherwise selected and the overall model is validated via literature data. Nevertheless, it is sufficiently accurate for a techno-economic assessment as executed during the present work.

In the context of waste heat recovery and supply to a DH network, a simplified strategy is implemented to estimate the potential of this concept. The economic viability assessment neglects the cost of piping or additional required pumps besides the related costs of the mentioned heat components. For the electrical demand of the heat pump, a constant COP is used, bypassing a detailed temperature demand profile of the DH system. Additionally, as with hydrogen production, no storage element is included for heat, further simplifying the system's dynamics.

3 Results and Discussion

3.1 Model Validation and Degradation

For an accurate simulation of PEM electrolysers, a validation process for the integrated electrolysis model (detailed in section 2.2) is crucial. Therefore, the characteristic polarisation curve ($i - V_{cell}$) of a single PEM cell was generated and subsequently compared to experimental data points presented in [48]. As mentioned in section 2.2.1, the anodic charge transfer coefficient was initially kept variable due to the dissimilarities within literature. It was determined that a value of 0.8 for α_{an} yielded optimal results, ensuring that the polarisation curve of the single cell under comparable operating conditions closely matched the data. The resulting value of α_{an} is in range with literature (see section 2.2.1), typically reporting 0-2 for the anodic CTC [67]. Figure 3.1 portrays the results of the process as well as the temperature dependency of the cell voltage.

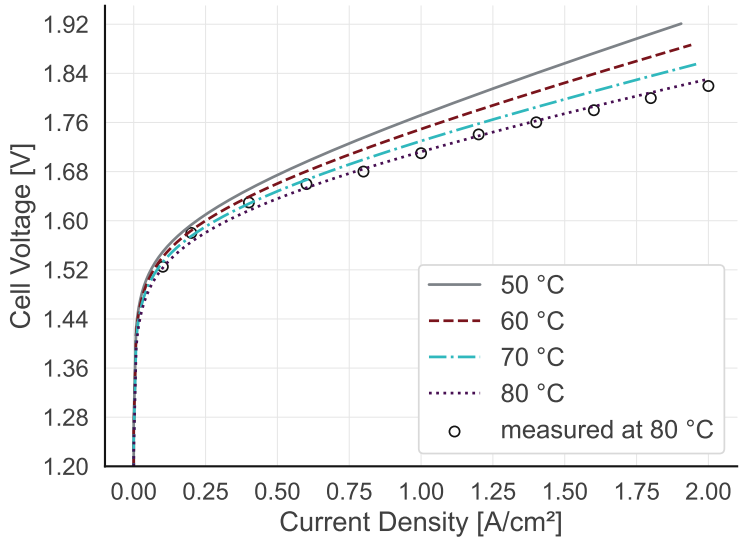

Figure 3.1: Simulated polarisation curve including data points from [48]

To further justify the proposed model, the nominal hydrogen production rate for the utilised 10 MW stack was determined at 2218.8 Nm^3/h. Additionally, the nominal current density and stack efficiency were calculated, at 3.46 A/cm^2 and 78.6 %, re-

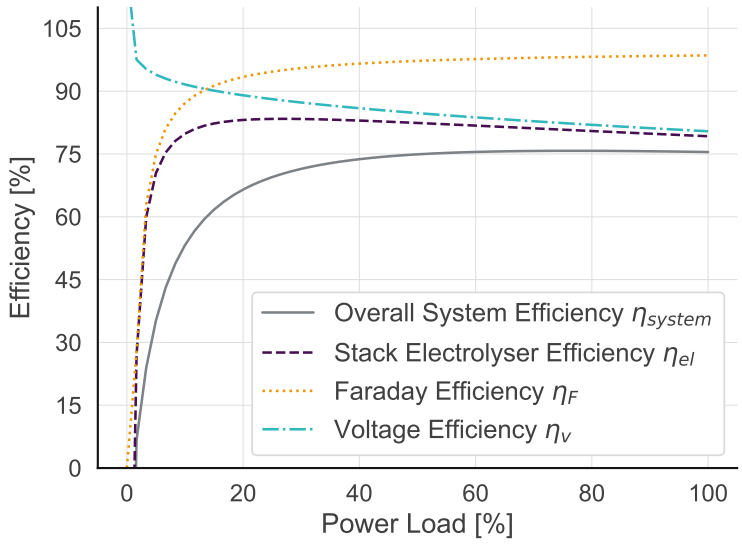

Figure 3.2: Efficiency of the investigated system at 80 °C

spectively. These stack parameters were evaluated under pressure and temperature conditions comparable to those reported in [12], with deviations remaining within 2 % and therefore confirming the model's reliability and suitability.

In Figure 3.2 the typical efficiency curve of an electrolyser is visualised, showing different efficiencies as a function of the power load of the electrolyser system. As explained in section 2.2, the stack electrolyser efficiency is the product of faraday and voltage efficiency. The critical metric for operation, however, is the overall system efficiency, which accounts for auxiliary losses that are not captured in other efficiency variations. Furthermore, electrolyser operation is generally limited to a specific minimum partial load to maintain gas purity [14, 45, 78]. Additional justification for this and the defined operational strategy (section 2.1.1) is provided by the fact that efficiency tends to drop significantly below approximately 20 % load. Notably, the efficiency of the electrolyser stack reaches its maximum around 25-30 % load and remains relatively stable at higher loads.

Due to the simulation duration, degradation is a crucial part within the utilised electrolyser model (see section 2.2) and its estimated effect on the polarisation curve is portrayed in Figure 3.3. As modelled, the degradation of cell voltage is directly proportional to the current density. The required cell voltage progressively increases as the electrolyser ages, reaching its peak after 80 000 h of operation. Across the entire simulation timespan of 20 years, the voltage degradation results in an average efficiency degradation of 1.33 %/a, which aligns appropriately with reported literature values ranging from 0.5-2.5 %/a [14, 30, 91].

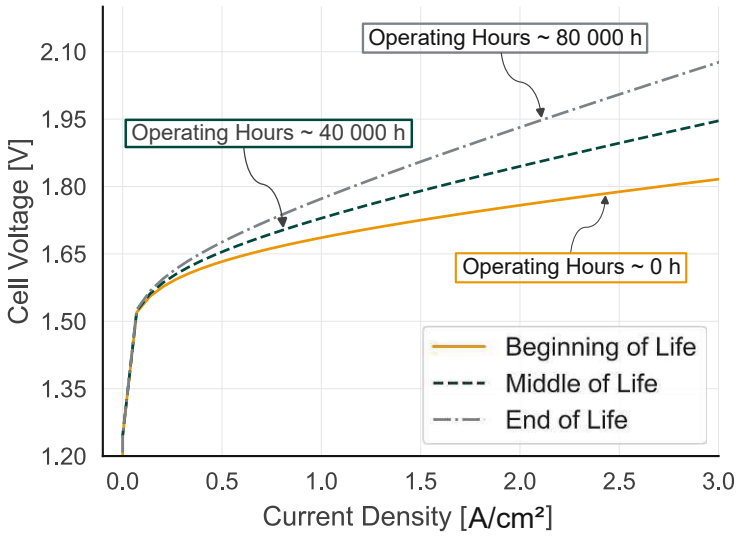

Figure 3.3: Simulated polarisation curve over time visualising degradation

3.2 Visualisation of Simulation and PEM Cooling Mechanism

As mentioned before, a simulation of an electrolyser system was at the core of this work. Here, Figure 3.4 provides an overview of simulation results characteristic for different seasons, additionally offering insights into the cooling mechanism, implemented as detailed in section 2.2.2. For this specific analysis plot, no additional electricity was supplied from the grid for continuous operation in contrast to the main simulation to particularly showcase the cooling strategy. The portrayed system configuration consists of a 100 MW PEM electrolyser system, with a combined renewable generation capacity of 200 MW. Due to the solar-powered aspect of the PV plant (amounts to 100 MW), hydrogen production is lower during the winter and adjoining months, as seen in the top subplot of Figure 3.4. The middle plot visually displays the current temperature state of both the electrolyser and the outlet cooling liquid, while the lowest of the three subplots outlines various heat fractions of the component evolving over time. If cooling is activated and consequently Q_{cool} is not equal to zero, the outlet liquid has a temperature of 65 °C, this value correlates to minimum supply temperatures of newer district heating networks in Austria (see section 1.1.3). The target temperature of the electrolyser is set to 80 °C, which is largely reached during operation. Comparatively, during shut down times (only existent in this particular simulation) the electrolyser cools down in correlation to lost thermal energy Q_{lost}. Once operation starts, the electrolyser is heated up by its own excess heat Q_{gen}, resulting in small temperature peaks at the beginning of

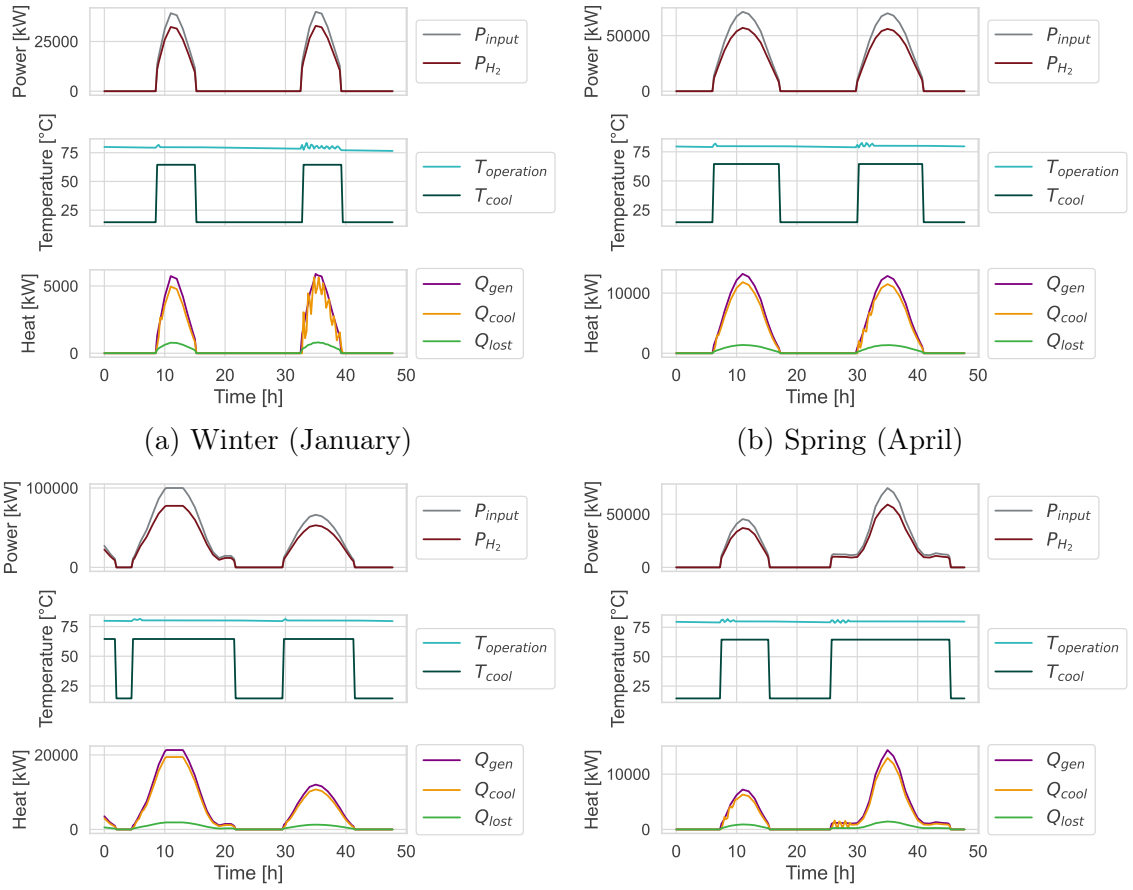

(a) Winter (January)

(b) Spring (April)

(c) Summer (July)

(d) Autumn (October)

Figure 3.4: Typical simulation results of selected parameters for different seasons of the year

each phase of hydrogen production. Temperature fluctuations (as depicted especially in Figure 3.4a and 3.4d) occur if the control mechanism of the cooling liquid - presently a PID-controller - does not immediately result in the designated operation temperature. However, the presented results show that typically the temperature is reached in sufficient time (e.g. shown in Figure 3.4b and 3.4c) and the fluctuations are not extensive, resulting in an adequate cooling mechanism for a techno-economic analysis.

3.3 KPI Results across various System Configurations

The results of three major KPIs and their dependency on the installed renewable capacity are displayed in Figure 3.5 for a *base-load* scenario (defined in section 2.1.1). The PV capacity as well as the wind capacity were varied between 0-140 MW, the

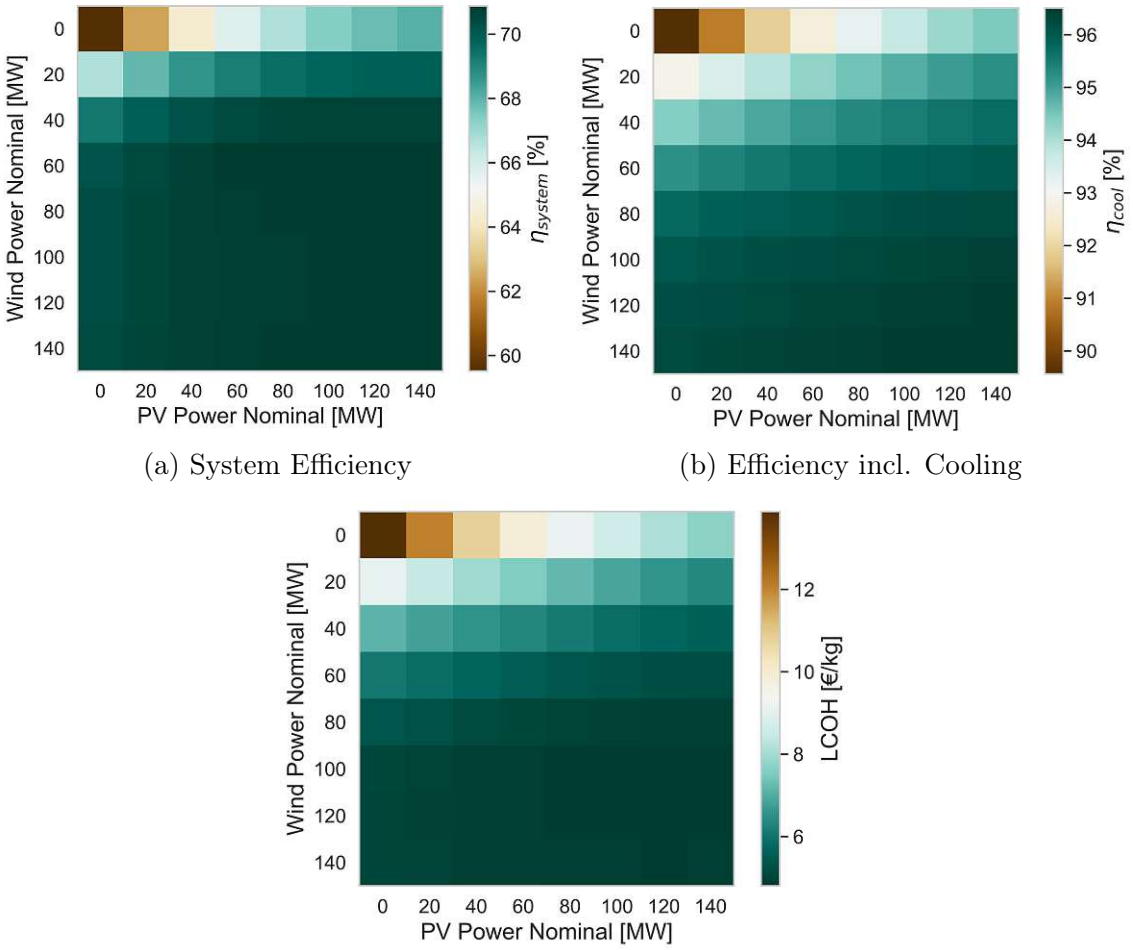

(a) System Efficiency

(b) Efficiency incl. Cooling

(c) LCOH

Figure 3.5: Analyses of KPIs depending on the combination of PV and electrolyser capacity

electrolyser having a size of 100 MW. A common trend observed is that higher renewable electricity generation leads to improved KPI values for the ones presented. The top left graphic 3.5a shows the system efficiency of the complete electrolyser system. As depicted, the highest estimated η_{system}, averaged over the simulation period, remains significantly below the maximum stack efficiency η_{el} at roughly 70 % (see section 3.1). This dissimilarity arises from the inclusion of auxiliary electricity consumption, which becomes particularly prominent during low partial load operation, see Figure 3.2. This correlation additionally explains the relatively rapid improvement of this KPI with rising renewable capacity.

The second KPI displayed is η_{cool} in Figure 3.5b. This particular efficiency hereby demonstrates the potential in efficiency enhancement, if the total extracted excess heat from the electrolysis process were to be used. The best configurations result in

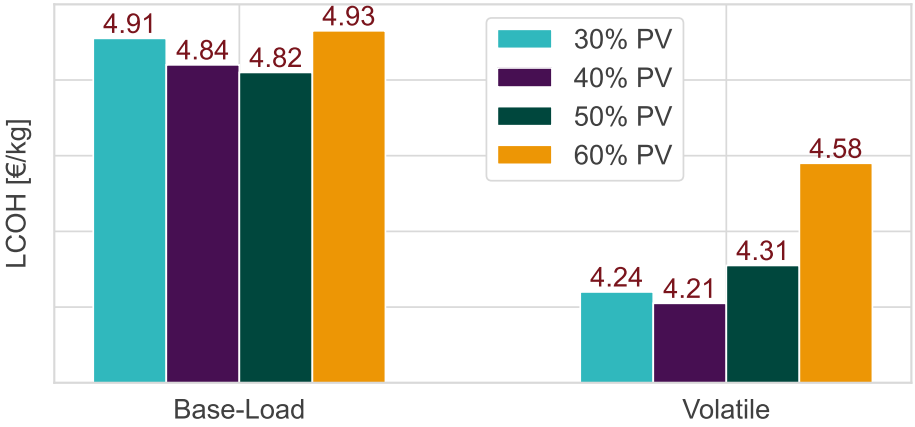

Figure 3.6: LCOH depending on scenarios; X% PV share of total renewable capacity equals 1-X% Wind

a value of approximately 96 %, effectively nearly 20 % points higher than solely the electrolyser stack efficiency. η_{el} is higher at partial load operation (see Figure 3.2), correlating to less excess heat production. As a result, η_{cool} decreases with reduced electricity input, presenting a behaviour opposite to that of stack efficiency. Furthermore, the identified efficiency gain aligns reasonably well with findings by Jonsson & Miljanovic [65], where an improved efficiency of 94.7 % could be achieved. Comparable results for overall efficiency including waste heat recovery are additionally concluded by Frank et al.' [92] and Burrin et al.' [18].

The final heatmap, along with Figure 3.6, illustrates the Levelised Cost of Hydrogen (LCOH). As shown in Figure 3.5c, favourable system configurations typically achieve an LCOH of approximately 4.8 €/kg, whereas scenarios with limited renewable energy generation can see costs rise to 10 €/kg or higher. The advantageous trend with increased renewable capacity is closely linked to the full load hours of the electrolyser, which inherently also rise with more available electricity. One of the most suitable configurations (120 MW Wind and 80 MW PV) reaches roughly 5300 FLH per simulated year. This result was calculated at an electrolyser size of 100 MW, but it was found that, generally, estimated KPIs are not dependent on the chosen electrolyser as all connected parameters are sized in relation to its capacity (PV, wind and converter capacity, grid electricity supply, etc.).

As implied above, an optimal system configuration emerges when the renewable generation capacity is double the installed electrolyser capacity. With this setup, Figure 3.6 provides a more in-depth analysis of the impact of the operational strategy - *base-load* vs. *volatile* (refer to section 2.1.1). Evidently, hydrogen production

costs are generally lower for the latter scenario, ranging from around 4.2 to 4.6 €/kg as opposed to 4.8-4.9 €/kg for a *base-load* operation. A trend for improved results with higher wind capacities compared to the PV equivalent is additionally visible, which is presumably correlated to the high full load hours of the wind profile - around 4080 FLH. LCOH values are minimised when the PV share constitutes approximately 40 % of the total installed renewable capacity, achieving the best results with a *volatile* scenario. Notably, this configuration also nearly represents the optimal setup for the *base-load* strategy and has therefore been frequently used as a reference throughout this work.

3.4 Significance of Electrolyser Capital Costs

As outlined in section 2.4, electrolyser CAPEX values vary widely, introducing a rather uncertain factor with significant contribution to the LCOH (see section 3.5 below). To address this, a sensitivity analysis was conducted to assess the impact of PEM capital expenditures on hydrogen production costs, with the results illustrated in Figure 3.7. The analysis reveals a linear correlation between capital costs and derived LCOH, with the *volatile* scenario yielding lower costs across the examined CAPEX range 200-2400 €/kW. Moreover, this strategy exhibits a slightly steeper slope, indicating that varied capital costs have a marginally bigger impact on the LCOH in this scenario. Lower overall electricity costs associated with this operational strategy are likely responsible for this observed link, amplifying the sensitivity of LCOH to CAPEX deviations.

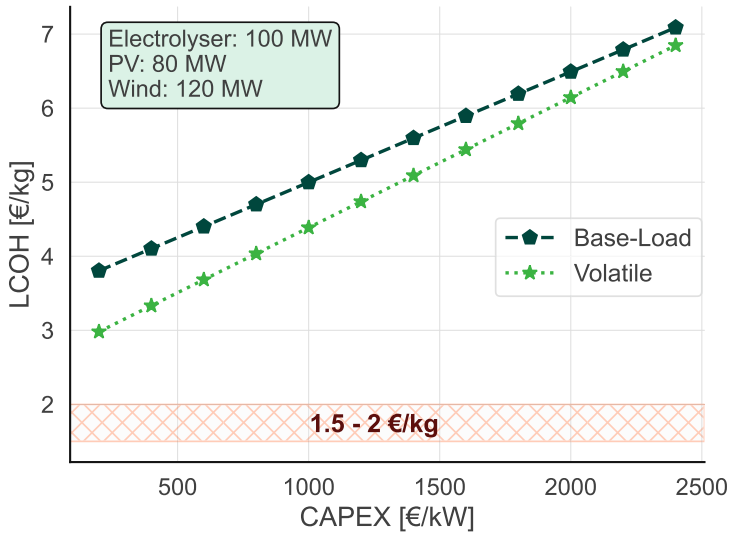

Figure 3.7: CAPEX Sensitivity Analysis, highlighting the target for global LCOH competitiveness (red horizontal bar)

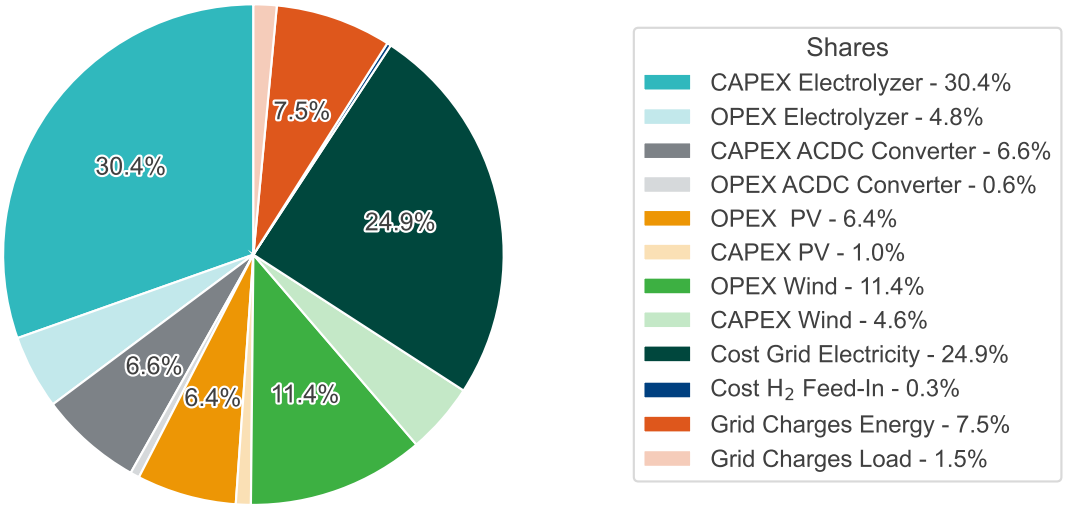

Figure 3.8: LCOH Cost Distribution

The Levelised Cost of Hydrogen presented ranges from approximately 3 to 7€/kg, increasing gradually with higher capital expenditures. While the lower values appear promising in comparison to current european hydrogen costs (refer to section 1.1.1 for H_2 costs), the maximum calculated LCOH numbers, based on industry-estimated CAPEX values, remain significantly higher than grey hydrogen production costs. The threshold for global competitive hydrogen production is indicated as a red horizontal bar in the graphic, and it is evident that even for optimistic futuristic CAPEX scenarios, the required LCOH values are out of reach. Therefore, it is questionable whether green hydrogen production can be economically viable worldwide under examined current conditions, unless the LCOH of fossil-based hydrogen increases.

3.5 Cost Breakdown of Levelised Cost of Energy

Various cashflow components (described in section 2.4) contribute to the determined Levelised Cost of Energy. For the LCOH, Figure 3.8 shows a pie chart illustrating the distribution of all factors and respective shares. As expected, the electrolyser CAPEX is one of the largest contributors, accounting for nearly a third of total costs. However, expenses related to electricity supplied from the grid are even slightly higher in this *base-load* scenario, additionally representing approximately one third overall. Here, the majority of costs (24.9 %) are correlated to the actual energy price of bought electricity, but remarkably grid connection charges are not negligible, amounting to 9 %. Moreover, other capital expenditures as well the OPEX of the electrolysis system further depict relevant contributions to the hydrogen production cost. Following these findings, it becomes evident that a significant reduction

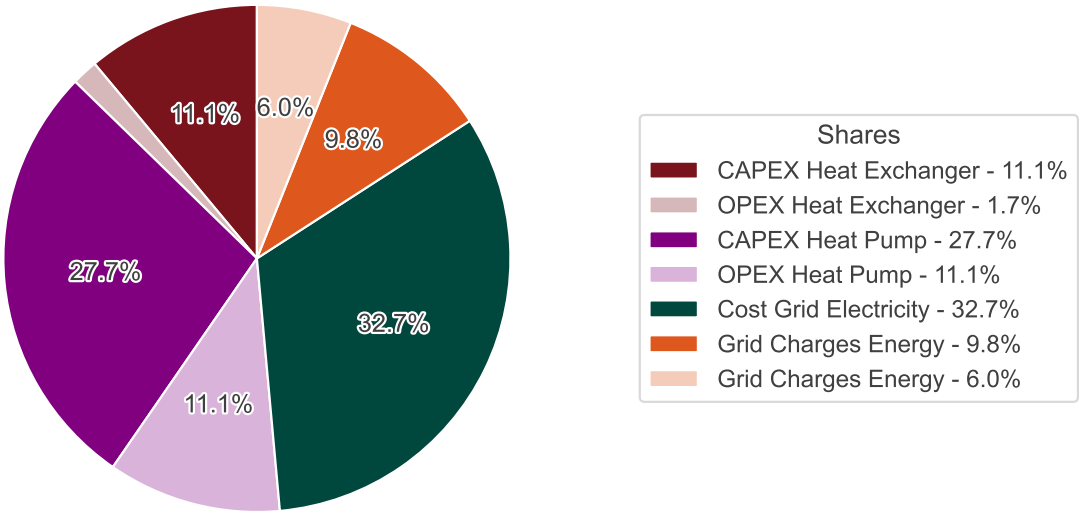

Figure 3.9: LCOHeat Cost Distribution

of the LCOH is most promising if either capital costs (see section 3.4) or grid electricity expenses can be minimised. The latter is confirmed by implementing the *volatile* strategy, where externally supplied electricity costs only contribute around 5.5 %. Regarding PEM electrolyser capital expenditures, reducing BoP-related costs is crucial [27, 32], alongside utilising innovation to lower expenses associated with stack components. Notably, the greatest cost reduction potential resides with the bipolar plates and porous transport layers in the stack [26, 32, 53, 58]. The extensive scaling-up process of PEM electrolysis systems is anticipated to aid with these challenges.

Furthermore, in Figure 3.9 the cost distribution for the Levelised Cost of Heat is displayed. By a considerable margin, the most significant contribution to the cost of supplying heat is the required heat pump and related expenses - substantiated by outcomes in [30] and [93]. The largest factor (32.7 %) is the cost of electricity necessary to power the HP, closely followed by its CAPEX. Additional costs include grid charges and operational expenditures of the heat pump. Expenses unrelated to the heat pump are attributed to the heat exchanger, accounting merely for approximately one eighth of all costs. The resulting LCOHeat values are thereafter listed and discussed in section 3.6.3.

3.6 Waste Heat Recovery and Supply

3.6.1 Analysis of Supply to Local District Heating Network

As defined before (section 2.3.1), supply of the electrolysis waste heat to a specific rural district heating network is modelled throughout the simulation. A particular KPI parameter - η_{DH} - subsequently represents the total efficiency of the PEM system including the useable thermal energy that can be provided. Results, summarised in Table 3.1, reveal that the overall efficiency shows only a marginal improvement compared to stack efficiency η_{el} - approximately 0.4 %. This limited enhancement is primarily due to the characteristics of the chosen DH network, which is both rural and relatively small, with peak demands of 0.65 MW, compared to the electrolyser's capacity. Indeed, the yearly heat demand of the network represents only roughly 1.5 % of the total extracted electrolysis excess heat (100 MW setup). Thus, the observed minimal efficiency improvement aligns with expectations, along with the nearly 100 % fulfilment of heat demand α_{load}. The latter further justifies the assumption made previously to directly consider the DH heat demand as input for heat pump calculations.

	Operational Strategy	
	Base-Load	***Volatile***
η_{el} [%]	76.13	76.38
η_{DH} [%]	76.44	76.75
α_{load} [%]	99.99	99.99

Table 3.1: Technical KPI Results related to Waste Heat Recovery; 40 % PV Share of Renewable Capacity

3.6.2 Potential of Heat Sales

Selling heat to the district heating network can also contribute to reducing the hydrogen cost. The LCOH, as described in section 2.4, was also calculated by incorporating the revenue generated from supplying useable thermal energy. Figure 3.10 illustrates the relative improvement of the LCOH, comparing the original LCOH with the reduced LCOH for a specific scenario. The analysis differentiates between operational strategies (*base-load* and *volatile*) and the assumed heat revenue per energy unit (either optimistic or pessimistic). As anticipated, the values associated with actual DH supply are extremely low. Additionally, the theoretical potential from heat sales derived from complete repurposing of useable waste heat is shown. The observed improvement ranges from 5.3-9.5 %, supported by findings in [38]. No-

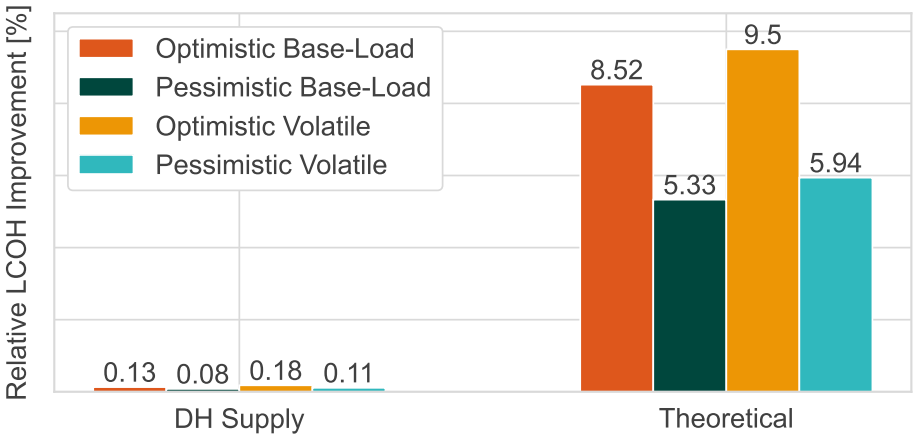

Figure 3.10: Relative LCOH Reductions via Heat Sales

tably, the *volatile* scenarios, especially when paired with the optimistic heat income assumptions, yield better results, with the latter being the dominant factor.

3.6.3 Viability

To justify waste heat recovery and its provision to DH networks, it is essential to check its viability by determining the Levelised Cost of Heat, as described in section 2.4. Under a *base-load* strategy, the LCOHeat is 45.41 €/MWh, while under a *volatile* strategy, the cost for supplying heat rises to 55.25 €/MWh. These results are based on the typical reference configuration (Electrolyser: 100 MW, Wind: 120 MW, PV: 80 MW) and align reasonably with selected literature values. Meriläinen et al.' reported costs up to 44 €/MWh [93] and Saranpää concluded a maximum of 59.4 €/MWh [94]. These sources as well as [30] additionally underline the high fluctuation of this parameter depending on the analysed scenario. Within the present work, costs increase significantly when renewable production decreases, likely due to the growing reliance on grid electricity, which represents a substantial portion of the LCOHeat cost (see section 3.5). A comparison of the estimated LCOHeat values with the defined heat profits clearly shows that supplying waste heat to the rural DH network is not financially viable. However, if the supply temperatures of the district heating network (e.g. a new generation DH system) match the direct output temperatures from the electrolyser, eliminating the need for a heat pump, the resulting LCOHeat drops to 3.88 €/MWh. This reduced cost then aligns easily with a feasible excess heat supply.

4 Conclusions and Outlook

This thesis investigated the techno-economic potential of a green hydrogen production plant in eastern Austria, powered by renewable energy sources and centred around a large-scale PEM electrolyser. The analysis focused on the period from 2030 to 2050, with operational strategies that include utilising a grid connection to ensure continuous H_2 production. The hydrogen production cost and its dependencies were explored in detail, followed by an examination of the technical and economic aspects of waste heat recovery from the electrolysis process and its potential for supplying thermal energy to a local district heating network. A PEM electrolysis model was additionally developed to conduct the simulation, with its validity confirmed through literature data.

The implemented model, encompassing an electrochemical and a thermal part, aligns well with literature and effectively simulates a PEM system with sufficient accuracy. It includes a fitted anodic CTC of 0.8 and accurately reflects the characteristics of the utilised 10 MW stack as well as the degradation of cell voltage, constituting 1.05 % points of annual decrease of efficiency. Moreover, a cooling mechanism ensures that the target temperature remains relatively stable, with only minor fluctuations observed.
This study demonstrates improved KPI results with high renewable energy generation, particularly in wind-heavy setups, achieving system efficiencies of up to 70 % under optimal conditions. Furthermore, repurposing waste heat has the theoretical potential to enhance electrolyser stack efficiency by nearly 20 % points, culminating in a total efficiency of approximately 96 %. The lowest LCOH values attained in this analysis range from 4.2-4.8 €/kg, with minimal costs observed under a *volatile* operational strategy that favours purchasing less, but more expensive grid electricity. This work further highlights that the LCOH is significantly influenced by electrolyser capital costs as well as grid supply expenses. A sensitivity analysis reveals that even in most optimistic CAPEX scenarios, green hydrogen costs struggle to compete with grey hydrogen, particularly on a global scale.
Findings of this work additionally reveal the potential of selling theoretically recoverable excess heat, as this could lead to an LCOH reduction of up to nearly 10 %. However, the limited capacity of the selected rural district heating network reduces

the effectiveness of waste heat recovery, yielding only marginal improvements in electrolyser efficiency and minor obtainable LCOH reductions. Nevertheless, a total coverage of the DH heat demand can be provided by the electrolysis plant, without necessitating heat storage. Economically, the viability of recycling excess heat remains uncertain as LCOHeat values are 45 €/MWh and 55 €/MWh for ideal configurations, respectively. These relatively high costs are primarily attributed to heat pump related expenses. Consequently, if the direct electrolysis output temperature is adequate for the intended application, heat supply becomes feasible, with costs reducing to 3.88 €/MWh.

To conclude, results of this study suggest that PEM electrolysis holds significant promise for future green hydrogen production, yet its associated production costs must still decrease substantially before it can become economically viable for widespread global deployment. Achieving competitiveness in the hydrogen market will depend on several factors. One of the most significant factors influencing the reduction of LCOH is the continued advancement of research and innovation with the objective of reducing the capital expenditures associated with PEM technology. Moreover, the introduction of carbon taxes could encourage the adoption of green hydrogen by making it, in comparison to fossil-based hydrogen, more economically attractive. Additionally, a reduction in supplementary (e.g. grid) electricity expenses, would significantly reduce costs, thus improving the overall economic outlook of H_2 production via PEM electrolysis.
Further analysis could refine presented LCOH estimates by considering more detailed electricity price structures, incorporating realistic fluctuations in market prices and thus optimising extra electricity purchases. Also the usage of storage systems, such as batteries, could minimise electricity procurement costs by perfecting the use of installed renewable capacities and mitigating the impact of intermittent electricity generation.
Ultimately, a more thorough investigation into the potential for waste heat recovery appears promising, as it could present an opportunity to further reduce hydrogen production costs through increased system efficiency and generating heat profits. Future research exploring various scenarios - considering factors such as electricity supply for the heat pump, district heating temperature profiles, transportation costs, and the integration of heat storage systems - would be valuable, as these aspects could influence the feasibility of heat repurposing. By systematically addressing variables indicated above, studies may unlock significant reductions in LCOH, potentially making green hydrogen production using PEM electrolysis a competitive alternative to grey hydrogen.

References

[1] M. Kayfeci, A. Keçebaş, and M. Bayat. "Hydrogen production". In: *Solar Hydrogen Production*. Elsevier, 2019, pp. 45–83. DOI: 10.1016/B978-0-12-814853-2.00003-5.

[2] J. M. Bermudez and S. Evangelopoulou. *Hydrogen*. Ed. by IEA International Energy Agency. 2023. URL: https://www.iea.org/energy-system/low-emission-fuels/hydrogen (last accessed 11/08/2024).

[3] Á. Hernández-Gómez, V. Ramirez, and D. Guilbert. "Investigation of PEM electrolyzer modeling: Electrical domain, efficiency, and specific energy consumption". *International Journal of Hydrogen Energy* 45 (2020), pp. 14625–14639. DOI: 10.1016/j.ijhydene.2020.03.195.

[4] IEA International Energy Agency, ed. *Global Hydrogen Review 2024*. 2024. URL: https://www.iea.org/reports/global-hydrogen-review-2024 (last accessed 11/08/2024).

[5] H. Nami, O. B. Rizvandi, C. Chatzichristodoulou, P. V. Hendriksen, and H. L. Frandsen. "Techno-economic analysis of current and emerging electrolysis technologies for green hydrogen production". *Energy Conversion and Management* 269 (2022), p. 116162. DOI: 10.1016/j.enconman.2022.116162.

[6] European Commission, ed. *Hydrogen*. 2024. URL: https://energy.ec.europa.eu/topics/energy-systems-integration/hydrogen_en (last accessed 11/08/2024).

[7] Federal Ministry Republic of Austria Labour and Economy, ed. *Hydrogen Strategy for Austria*. 2022. URL: https://www.bmaw.gv.at/en/Topics/International/Hydrogen-Strategy-for-Austria (last accessed 11/08/2024).

[8] B. S. Zainal, P. J. Ker, H. Mohamed, H. C. Ong, I. Fattah, S. A. Rahman, L. D. Nghiem, and T. M. I. Mahlia. "Recent advancement and assessment of green hydrogen production technologies". *Renewable and Sustainable Energy Reviews* 189 (2024), p. 113941. DOI: 10.1016/j.rser.2023.113941.

[9] T. Terlouw, C. Bauer, R. McKenna, and M. Mazzotti. "Large-scale hydrogen production via water electrolysis: a techno-economic and environmental assessment". *Energy & Environmental Science* 15 (2022), pp. 3583–3602. DOI: 10.1039/D2EE01023B.

[10] F. Pavan, J. M. Bermudez, S. Evangelopoulou, and S. Bennett. *Electrolysers*. Ed. by IEA International Energy Agency. 2023. URL: https://www.iea.org/energy-system/low-emission-fuels/electrolysers (last accessed 11/11/2024).

[11] M. Nasser, T. F. Megahed, S. Ookawara, and H. Hassan. "A review of water electrolysis-based systems for hydrogen production using hybrid/solar/wind energy systems". *Environmental science and pollution research international* 29 (2022), pp. 86994–87018. DOI: 10.1007/s11356-022-23323-y.

[12] H. van 't Noordende and P. Ripson. *A One-GigaWatt Green-Hydrogen Plant: Advanced Design and Total Installed-Capital Costs*. Ed. by Christa de Ruyter. 2022. URL: https://ispt.eu/media/Public-report-gigawatt-advanced-green-electrolyser-design.pdf (last accessed 06/24/2024).

[13] J. Chi and H. Yu. "Water electrolysis based on renewable energy for hydrogen production". *Chinese Journal of Catalysis* 39 (2018), pp. 390–394. DOI: 10.1016/S1872-2067(17)62949-8.

[14] A. Buttler and H. Spliethoff. "Current status of water electrolysis for energy storage, grid balancing and sector coupling via power-to-gas and power-to-liquids: A review". *Renewable and Sustainable Energy Reviews* 82 (2018), pp. 2440–2454. DOI: 10.1016/j.rser.2017.09.003.

[15] K. Ayers, N. Danilovic, K. Harrison, and H. Xu. "PEM Electrolysis, a Forerunner for Clean Hydrogen". *The Electrochemical Society Interface* 30 (2021), pp. 67–72. DOI: 10.1149/2.F16214IF.

[16] Hydrogen and Fuel Cell Technologies Office. *Hydrogen Production: Electrolysis*. Ed. by Office of Energy Efficiency & Renewable Energy. 2024. URL: https://www.energy.gov/eere/fuelcells/hydrogen-production-electrolysis (last accessed 11/08/2024).

[17] H. Böhm, S. Moser, S. Puschnigg, and A. Zauner. "Power-to-hydrogen & district heating: Technology-based and infrastructure-oriented analysis of (future) sector coupling potentials". *International Journal of Hydrogen Energy* 46 (2021), pp. 31938–31951. DOI: 10.1016/j.ijhydene.2021.06.233.

[18] D. Burrin, S. Roy, A. P. Roskilly, and A. Smallbone. "A combined heat and green hydrogen (CHH) generator integrated with a heat network". *Energy Conversion and Management* 246 (2021), p. 114686. DOI: 10.1016/j.enconman.2021.114686.

[19] A. María Villarreal Vives, R. Wang, S. Roy, and A. Smallbone. "Techno-economic analysis of large-scale green hydrogen production and storage". *Applied Energy* 346 (2023), p. 121333. DOI: 10.1016/j.apenergy.2023.121333.

[20] P. Saha, F. A. Akash, S. M. Shovon, M. U. Monir, M. T. Ahmed, M. F. H. Khan, S. M. Sarkar, M. K. Islam, M. M. Hasan, D.-V. N. Vo, A. A. Aziz, M. J. Hossain, and R. Akter. "Grey, blue, and green hydrogen: A comprehensive review of production methods and prospects for zero-emission energy". *International Journal of Green Energy* 21 (2024), pp. 1383–1397. DOI: 10.1080/15435075.2023.2244583.

[21] J. M. M. Arcos and D. M. F. Santos. "The Hydrogen Color Spectrum: Techno-Economic Analysis of the Available Technologies for Hydrogen Production". *Gases* 3 (2023), pp. 25–46. DOI: 10.3390/gases3010002.

[22] IRENA International Renewable Energy Agency, ed. *Hydrogen*. 2022. URL: https://www.irena.org/Energy-Transition/Technology/Hydrogen (last accessed 11/13/2024).

[23] S. Shiva Kumar and V. Himabindu. "Hydrogen production by PEM water electrolysis – A review". *Materials Science for Energy Technologies* 2 (2019), pp. 442–454. DOI: 10.1016/j.mset.2019.03.002.

[24] European Hydrogen Observatory, ed. *Cost of hydrogen production*. 2024. URL: https://observatory.clean-hydrogen.europa.eu/hydrogen-landscape/production-trade-and-cost/cost-hydrogen-production (last accessed 11/13/2024).

[25] IRENA International Renewable Energy Agency, ed. *Making the Breakthrough: Green hydrogen Green hydrogen policies and technology costs*. 2021. URL: https://www.irena.org/-/media/Files/IRENA/Agency/Publication/2020/Nov/IRENA_Green_Hydrogen_breakthrough_2021.pdf (last accessed 11/13/2024).

[26] K. Zhang, X. Liang, L. Wang, K. Sun, Y. Wang, Z. Xie, Q. Wu, X. Bai, M. S. Hamdy, H. Chen, and X. Zou. "Status and perspectives of key materials for PEM electrolyzer". *Nano Research Energy* 1 (2022), e9120032. DOI: 10.26599/NRE.2022.9120032.

[27] H. Sayed-Ahmed, Á. Toldy, and A. Santasalo-Aarnio. "Dynamic operation of proton exchange membrane electrolyzers—Critical review". *Renewable and Sustainable Energy Reviews* 189 (2024), p. 113883. DOI: 10.1016/j.rser.2023.113883.

[28] D. S. Falcão and A. Pinto. "A review on PEM electrolyzer modelling: Guidelines for beginners". *Journal of Cleaner Production* 261 (2020), p. 121184. DOI: 10.1016/j.jclepro.2020.121184.

[29] O. Ulleberg. "Modeling of advanced alkaline electrolyzers: a system simulation approach". *International Journal of Hydrogen Energy* 28 (2003), pp. 21–33. DOI: 10.1016/S0360-3199(02)00033-2.

[30] E. van der Roest, R. Bol, T. Fens, and A. van Wijk. "Utilisation of waste heat from PEM electrolysers – Unlocking local optimisation". *International Journal of Hydrogen Energy* 48 (2023), pp. 27872–27891. DOI: 10.1016/j.ijhydene.2023.03.374.

[31] R. Hancke, P. Bujlo, T. Holm, and Ø. Ulleberg. "High-pressure PEM water electrolyser performance up to 180 bar differential pressure". *Journal of Power Sources* 601 (2024), p. 234271. DOI: 10.1016/j.jpowsour.2024.234271.

[32] IRENA International Renewable Energy Agency, ed. *Green Hydrogen Cost Reduction: Scaling up Electrolysers to Meet the 1.5 C Climate Goal*. 2020. URL: https://www.irena.org/-/media/Files/IRENA/Agency/Publication/2020/Dec/IRENA_Green_hydrogen_cost_2020.pdf (last accessed 11/22/2024).

[33] U.S. Department of Energy, ed. *Critical Materials Assessment*. 2023. URL: https://www.energy.gov/sites/default/files/2023-07/doe-critical-material-assessment_07312023.pdf (last accessed 08/08/2024).

[34] C. Minke, M. Suermann, B. Bensmann, and R. Hanke-Rauschenbach. "Is iridium demand a potential bottleneck in the realization of large-scale PEM water electrolysis?" *International Journal of Hydrogen Energy* 46 (2021), pp. 23581–23590. DOI: 10.1016/j.ijhydene.2021.04.174.

[35] e-think. Zentrum für Energiewirtschaft und Umwelt, ed. *Austrian Heat Map*. URL: https://austrian-heatmap.gv.at/karte/.

[36] M. Köfinger, D. Basciotti, R. R. Schmidt, E. Meissner, C. Doczekal, and A. Giovannini. "Low temperature district heating in Austria: Energetic, ecologic and economic comparison of four case studies". *Energy* 110 (2016), pp. 95–104. DOI: 10.1016/j.energy.2015.12.103.

[37] E. Guelpa, M. Capone, A. Sciacovelli, N. Vasset, R. Baviere, and V. Verda. "Reduction of supply temperature in existing district heating: A review of strategies and implementations". *Energy* 262 (2023), p. 125363. DOI: 10.1016/j.energy.2022.125363.

[38] N. Frassl, N. R. Sistani, Y. Wimmer, J. Kapeller, K. Maggauer, and J. Kathan. "Techno-economic assessment of waste heat recovery for green hydrogen production: a simulation study". *e+i Elektrotechnik und Informationstechnik* 141 (2024), pp. 288–298. DOI: 10.1007/s00502-024-01231-y.

[39] O. Terreros, J. Spreitzhofer, D. Basciotti, R. R. Schmidt, T. Esterl, M. Pober, M. Kerschbaumer, and M. Ziegler. "Electricity market options for heat pumps in rural district heating networks in Austria". *Energy* 196 (2020), p. 116875. DOI: 10.1016/j.energy.2019.116875.

[40] A. Müller, R. Heimrath, F. Mauthner, C. Halmdienst, R. Büchele, L. Kranzl, and G. Totschnig. "Solarenergie und Wärmenetze: Optionen und Barrieren in einer langfristigen, integrativen Sichtweise" (2014).

[41] M. H. Abbasi, B. Abdullah, M. W. Ahmad, A. Rostami, and J. Cullen. "Heat transition in the European building sector: Overview of the heat decarbonisation practices through heat pump technology". *Sustainable Energy Technologies and Assessments* 48 (2021), p. 101630. DOI: 10.1016/j.seta.2021.101630.

[42] A. Marina, S. Spoelstra, H. A. Zondag, and A. K. Wemmers. "An estimation of the European industrial heat pump market potential". *Renewable and Sustainable Energy Reviews* 139 (2021), p. 110545. DOI: 10.1016/j.rser.2020.110545.

[43] E. Popovski, A. Aydemir, T. Fleiter, D. Bellstädt, R. Büchele, and J. Steinbach. "The role and costs of large-scale heat pumps in decarbonising existing district heating networks – A case study for the city of Herten in Germany". *Energy* 180 (2019), pp. 918–933. DOI: 10.1016/j.energy.2019.05.122.

[44] M. Jesper, F. Schlosser, F. Pag, T. G. Walmsley, B. Schmitt, and K. Vajen. "Large-scale heat pumps: Uptake and performance modelling of market-available devices". *Renewable and Sustainable Energy Reviews* 137 (2021), p. 110646. DOI: 10.1016/j.rser.2020.110646.

[45] D. Parra and M. K. Patel. "Techno-economic implications of the electrolyser technology and size for power-to-gas systems". *International Journal of Hydrogen Energy* 41 (2016), pp. 3748–3761. DOI: 10.1016/j.ijhydene.2015.12.160.

[46] N. K. Landin and B. C. Windom. "Evaluating the efficiency of a proton exchange membrane green hydrogen generation system using balance of plant modeling". *International Journal of Hydrogen Energy* 57 (2024), pp. 1273–1285. DOI: 10.1016/j.ijhydene.2024.01.128.

[47] P. Olivier, C. Bourasseau, and P. B. Bouamama. "Low-temperature electrolysis system modelling: A review". *Renewable and Sustainable Energy Reviews* 78 (2017), pp. 280–300. DOI: 10.1016/j.rser.2017.03.099.

[48] A. S. Tijani, M. A. Ghani, A. A. Rahim, I. K. Muritala, and F. A. Binti Mazlan. "Electrochemical characteristics of (PEM) electrolyzer under influence of charge transfer coefficient". *International Journal of Hydrogen Energy* 44 (2019), pp. 27177–27189. DOI: 10.1016/j.ijhydene.2019.08.188.

[49] B. Han, S. M. Steen, J. Mo, and F.-Y. Zhang. "Electrochemical performance modeling of a proton exchange membrane electrolyzer cell for hydrogen energy". *International Journal of Hydrogen Energy* 40 (2015), pp. 7006–7016. DOI: 10.1016/j.ijhydene.2015.03.164.

[50] M. Espinosa-López, C. Darras, P. Poggi, R. Glises, P. Baucour, A. Rakotondrainibe, S. Besse, and P. Serre-Combe. "Modelling and experimental validation of a 46 kW PEM high pressure water electrolyzer". *Renewable Energy* 119 (2018), pp. 160–173. DOI: 10.1016/j.renene.2017.11.081.

[51] W.J. Tiktak. "Heat Management of PEM Electrolysis: A study on the potential of excess heat from medium to largescale PEM electrolyisis and the performance analysis of a dedicated cooling system". Master Thesis. TU Delft, 2019.

[52] A. E. Samani, A. D'Amicis, J. D. de Kooning, D. Bozalakov, P. Silva, and L. Vandevelde. "Grid balancing with a large–scale electrolyser providing primary reserve". *IET Renewable Power Generation* 14 (2020), pp. 3070–3078. DOI: 10.1049/iet-rpg.2020.0453.

[53] S. Krishnan, V. Koning, M. Theodorus de Groot, A. de Groot, P. G. Mendoza, M. Junginger, and G. J. Kramer. "Present and future cost of alkaline and PEM electrolyser stacks". *International Journal of Hydrogen Energy* 48 (2023), pp. 32313–32330. DOI: 10.1016/j.ijhydene.2023.05.031.

[54] P. Fragiacomo and M. Genovese. "Modeling and energy demand analysis of a scalable green hydrogen production system". *International Journal of Hydrogen Energy* 44 (2019), pp. 30237–30255. DOI: 10.1016/j.ijhydene.2019.09.186.

[55] S. Metz, T. Smolinka, C. I. Bernäcker, S. Loos, T. Rauscher, L. Röntzsch, M. Arnold, A. L. Görne, M. Jahn, M. Kusnezoff, G. Kolb, U.-P. Apfel, and C. Doetsch. "Wasserstofferzeugung durch Elektrolyse und weitere Verfahren". In: *Wasserstofftechnologien*. Ed. by R. Neugebauer. Berlin, Heidelberg: Springer Berlin Heidelberg, 2022, pp. 207–258. DOI: 10.1007/978-3-662-64939-8_9.

[56] J. J. Caparrós Mancera, F. Segura Manzano, J. M. Andújar, F. J. Vivas, and A. J. Calderón. "An Optimized Balance of Plant for a Medium-Size PEM Electrolyzer: Design, Control and Physical Implementation". *Electronics* 9 (2020), p. 871. DOI: 10.3390/electronics9050871.

[57] Tom Smolinka. *Cost break down and analysis of PEM Cost break down and analysis of PEM electrolysis systems for different industrial and Power to Gas applications*. 2015. URL: https://publica-rest.fraunhofer.de/server/api/core/bitstreams/440df736-a426-45e3-8187-7e7f8b603046/content (last accessed 06/24/2024).

[58] M. Holst, S. Aschbrenner, T. Smolinka, C. Voglstätter, and G. Grimm. *Cost forecast for low-temperature electrolysis-technology driven bottom-up prognosis for PEM and alkaline water electrolysis systems*. 2021. URL: https://www.ise.fraunhofer.de/content/dam/ise/de/documents/publications/studies/cost-forecast-for-low-temperature-electrolysis.pdf (last accessed 08/09/2024).

[59] R. Hancke, T. Holm, and Ø. Ulleberg. "The case for high-pressure PEM water electrolysis". *Energy Conversion and Management* 261 (2022), p. 115642. DOI: 10.1016/j.enconman.2022.115642.

[60] H. Formayer, I. Nadeem, D. Leidinger, P. Maier, F. Schöniger, D. Suna, G. Resch, G. Totschnig, and F. Lehner. "SECURES-Met: A European meteorological data set suitable for electricity modelling applications". *Scientific data* 10 (2023), p. 590. DOI: 10.1038/s41597-023-02494-4.

[61] H. Formayer, P. Maier, I. Nadeem, D. Leidinger, F. Lehner, F. Schöniger, G. Resch, D. Suna, P. Widhalm, N. Pardo-Garcia, F. Hasengst, and G. Totschnig. *SECURES-Met - A European wide meteorological data set suitable for electricity modelling (supply and demand) for historical climate and climate change projections*. 2023. DOI: 10.5281/zenodo.7907883.

[62] S. Pezzutto, S. Zambotti, S. Croce, P. Zambelli, G. Garegnani, C. Scaramuzzino, R. Pascual Pascuas, A. Zubaryeva, F. Haas, Exner, Dagmar, Müller, Andreas, Hartner, Michael, T. Fleiter, A.-L. Klingler, M. Kühnbach, P. Manz, S. Marwitz, M. Rehfeldt, J. Steinbach, Popovski, Eftim (Fraunhofer ISI). Reviewed by Kranzl, Lukas, and S. (Fritz. *Hotmaps Project: D2.3 WP2 Report – Open Data Set for the EU28*. 2018. URL: www.hotmaps-project.eu (last accessed 11/28/2023).

[63] A. S. Tijani, N. A. Binti Kamarudin, and F. A. Binti Mazlan. "Investigation of the effect of charge transfer coefficient (CTC) on the operating voltage of polymer electrolyte membrane (PEM) electrolyzer". *International Journal of Hydrogen Energy* 43 (2018), pp. 9119–9132. DOI: 10.1016/j.ijhydene.2018.03.111.

[64] C. BIAKU, N. DALE, M. MANN, H. SALEHFAR, A. PETERS, and T. HAN. "A semiempirical study of the temperature dependence of the anode charge transfer coefficient of a 6kW PEM electrolyzer". *International Journal of Hydrogen Energy* 33 (2008), pp. 4247–4254. DOI: 10.1016/j.ijhydene.2008.06.006.

[65] Fredrik Jonsson and Andrea Miljanovic. "Utilization Of Waste Heat From Hydrogen Production: A case study on the Botnia Link H2 Project in Luleå, Sweden". Master Thesis. Mälardalen University, 2022.

[66] R. García-Valverde, N. Espinosa, and A. Urbina. "Simple PEM water electrolyser model and experimental validation". *International Journal of Hydrogen Energy* 37 (2012), pp. 1927–1938. DOI: 10.1016/j.ijhydene.2011.09.027.

[67] Z. Abdin, C. J. Webb, and E. Gray. "Modelling and simulation of a proton exchange membrane (PEM) electrolyser cell". *International Journal of Hydrogen Energy* 40 (2015), pp. 13243–13257. DOI: 10.1016/j.ijhydene.2015.07.129.

[68] E. Crespi, G. Guandalini, L. Mastropasqua, S. Campanari, and J. Brouwer. "Experimental and theoretical evaluation of a 60 kW PEM electrolysis system for flexible dynamic operation". *Energy Conversion and Management* 277 (2023), p. 116622. DOI: 10.1016/j.enconman.2022.116622.

[69] A. Majumdar, M. Haas, I. Elliot, and S. Nazari. "Control and control-oriented modeling of PEM water electrolyzers: A review". *International Journal of Hydrogen Energy* 48 (2023), pp. 30621–30641. DOI: 10.1016/j.ijhydene.2023.04.204.

[70] B. Yodwong, D. Guilbert, M. Phattanasak, W. Kaewmanee, M. Hinaje, and G. Vitale. "Faraday's Efficiency Modeling of a Proton Exchange Membrane Electrolyzer Based on Experimental Data". *Energies* 13 (2020), p. 4792. DOI: 10.3390/en13184792.

[71] T. Adibi, A. Sojoudi, and S. C. Saha. "Modeling of thermal performance of a commercial alkaline electrolyzer supplied with various electrical currents". *International Journal of Thermofluids* 13 (2022), p. 100126. DOI: 10.1016/j.ijft.2021.100126.

[72] R. Keller, E. Rauls, M. Hehemann, M. Müller, and M. Carmo. "An adaptive model-based feedforward temperature control of a 100 kW PEM electrolyzer". *Control Engineering Practice* 120 (2022), p. 104992. DOI: 10.1016/j.conengprac.2021.104992.

[73] R. Qi, J. Li, J. Lin, Y. Song, J. Wang, Q. Cui, Y. Qiu, M. Tang, and J. Wang. "Thermal modeling and controller design of an alkaline electrolysis system under dynamic operating conditions". *Applied Energy* 332 (2023), p. 120551. DOI: 10.1016/j.apenergy.2022.120551.

[74] Austrian Standards International, ed. *ÖNORM H 5056-1: Gesamtenergieeffizienz von Gebäuden*. 2019. URL: https://www.austrian-standards.at/de_copy/shop/onorm-h-5056-1-2019-01-15~p2455573 (last accessed 11/21/2024).

[75] A. H. Reksten, M. S. Thomassen, S. Møller-Holst, and K. Sundseth. "Projecting the future cost of PEM and alkaline water electrolysers; a CAPEX model including electrolyser plant size and technology development". *International Journal of Hydrogen Energy* 47 (2022), pp. 38106–38113. DOI: 10.1016/j.ijhydene.2022.08.306.

[76] J. Hemauer, S. Rehfeldt, H. Klein, and A. Peschel. "Performance and cost modelling taking into account the uncertainties and sensitivities of current and next-generation PEM water electrolysis technology". *International Journal of Hydrogen Energy* 48 (2023), pp. 25619–25634. DOI: 10.1016/j.ijhydene.2023.03.050.

[77] J. Proost. "State-of-the art CAPEX data for water electrolysers, and their impact on renewable hydrogen price settings". *International Journal of Hydrogen Energy* 44 (2019), pp. 4406–4413. DOI: 10.1016/j.ijhydene.2018.07.164.

[78] H. van 't Noordende and P. Ripson. *Baseline design and total installed costs of a GW green hydrogen plant: State-of-the-art design and total installed capital costs*. Ed. by Institute for Sustainable Process Technology. 2020. URL: https://ispt.eu/media/ISPT-public-report-gigawatt-green-hydrogen-plant.pdf (last accessed 06/06/2024).

[79] L. Sens, U. Neuling, and M. Kaltschmitt. "Capital expenditure and levelized cost of electricity of photovoltaic plants and wind turbines – Development by 2050". *Renewable Energy* 185 (2022), pp. 525–537. DOI: 10.1016/j.renene.2021.12.042.

[80] Adam Christensen. *Assessment of Hydrogen Production Costs from Electrolysis: United States and Europe*. 2020. URL: https://theicct.org/wp-content/uploads/2021/06/final_icct2020_assessment_of-_hydrogen_production_costs-v2.pdf (last accessed 11/19/2023).

[81] M. A. Semeraro. "Renewable energy transport via hydrogen pipelines and HVDC transmission lines". *Energy Strategy Reviews* 35 (2021), p. 100658. DOI: 10.1016/j.esr.2021.100658.

[82] S. Brynolf, M. Taljegard, M. Grahn, and J. Hansson. "Electrofuels for the transport sector: A review of production costs". *Renewable and Sustainable Energy Reviews* 81 (2018), pp. 1887–1905. DOI: 10.1016/j.rser.2017.05.288.

[83] M. Fasihi, R. Weiss, J. Savolainen, and C. Breyer. "Global potential of green ammonia based on hybrid PV-wind power plants". *Applied Energy* 294 (2021), p. 116170. DOI: 10.1016/j.apenergy.2020.116170.

[84] N. Fuchs, G. Jambrich, and H. Brunner. "Simulation Tool for Techno-economic Analysis of Hybrid AC/DC Low Voltage Distribution Grids". In: *CIRED 2021 - The 26th International Conference and Exhibition on Electricity Distribution*. Institution of Engineering and Technology, 2021, pp. 2549–2553. DOI: 10.1049/icp.2021.2122.

[85] P. Saini, P. Huang, F. fiedler, A. Volkova, and X. Zhang. "Techno-economic analysis of a 5th generation district heating system using thermo-hydraulic model: A multi-objective analysis for a case study in heating dominated climate". *Energy and Buildings* 296 (2023), p. 113347. DOI: 10.1016/j.enbuild.2023.113347.

[86] Y. Jovet, F. Lefèvre, A. Laurent, and M. Clausse. "Combined energetic, economic and climate change assessment of heat pumps for industrial waste heat recovery". *Applied Energy* 313 (2022), p. 118854. DOI: 10.1016/j.apenergy.2022.118854.

[87] Netz Burgenland, ed. *Preisblatt der Netz Burgenland GmbH, Bereich Strom*. 2024. URL: https://assets.netzburgenland.at/20240101_Preisblatt_Strombereich_gueltig_ab_1_1_2024_58d9837f57.pdf (last accessed 11/22/2024).

[88] J. Kathan, J. Kapeller, S. Reuter, P. Ortmann, A. Rodgarkia-Dara, M. Reger, G. Brändle, and C. Gatzen. *Importmöglichkeiten für erneuerbaren Wasserstoff*. Ed. by Bundesministerium für Klimaschutz, Umwelt, Energie, Mobilität, Innovation und Technologie. 2022. URL: https://www.bmk.gv.at/themen/energie/publikationen/importmoeglichkeiten.html (last accessed 11/22/2024).

[89] G. Bucar, K. Schweyer, C. Fink, R. Riva, M. Neuhäuser, E. Meissner, W. Streicher, and C. Halmdienst. *Dezentrale erneuerbare Energie für bestehende Fernwärmenetze*. Ed. by Bundesministerium für Verkehr, Innovation und Technologie. 2005. URL: https://www.nachhaltigwirtschaften.at/resources/edz_pdf/0678_dezentrale_energieerzeugung_fuer_fernwaerme.pdf (last accessed 10/27/2023).

[90] M. Saxe and P. Alvfors. "Advantages of integration with industry for electrolytic hydrogen production". *Energy* 32 (2007), pp. 42–50. DOI: 10.1016/j.energy.2006.01.021.

[91] M. Felgenhauer and T. Hamacher. "State-of-the-art of commercial electrolyzers and on-site hydrogen generation for logistic vehicles in South Carolina". *International Journal of Hydrogen Energy* 40 (2015), pp. 2084–2090. DOI: 10.1016/j.ijhydene.2014.12.043.

[92] E. Frank, J. Gorre, F. Ruoss, and M. J. Friedl. "Calculation and analysis of efficiencies and annual performances of Power-to-Gas systems". *Applied Energy* 218 (2018), pp. 217–231. DOI: 10.1016/j.apenergy.2018.02.105.

[93] A. Meriläinen, A. Kosonen, J. Jokisalo, R. Kosonen, P. Kauranen, and J. Ahola. "Techno-economic evaluation of waste heat recovery from an off-grid alkaline water electrolyzer plant and its application in a district heating network in Finland". *Energy* 306 (2024), p. 132181. DOI: 10.1016/j.energy.2024.132181.

[94] V. Saranpää. "Electrolyser waste heat utilization in district heating applications: Techno-economic optimization study". Master's Thesis. Aalto University, 2024.